ISTANBUL TECHNICAL UNIVERSITY ★ ENERGY INSTITUTE

NUMERICAL INVESTIGATION OF FLOW IN A CHANNEL WITH POROUS BAFFLES

M.Sc. THESIS

Ahmet BAŞ

Energy Science and Technology Division

Energy Science and Technology Programme

OCTOBER 2018

ISTANBUL TECHNICAL UNIVERSITY ★ ENERGY INSTITUTE

NUMERICAL INVESTIGATION OF FLOW IN A CHANNEL WITH POROUS BAFFLES

M.Sc. THESIS

Ahmet Baş
(301141030)

Energy Science and Technology Division

Energy Science and Technology Programme

Thesis Advisor: Prof. Dr. Filiz Baytaş

OCTOBER 2018

İSTANBUL TEKNİK ÜNİVERSİTESİ ★ ENERJİ ENSTİTÜSÜ

GÖZENEKLİ DUVARLAR BULUNAN BİR KANALDAKİ AKIŞIN SAYISAL İNCELEMESİ

YÜKSEK LİSANS TEZİ

Ahmet BAŞ
(301141030)

Enerji Bilim ve Teknoloji Anabilim Dalı

Enerji Bilim ve Teknoloji Programı

Tez Danışmanı: Prof. Dr. Filiz BAYTAŞ

EKİM 2018

Ahmet Baş, a M.Sc. student of ITU Institute of Energy student ID 301141030, successfully defended the thesis entitled "NUMERICAL INVESTIGATION OF FLOW IN A CHANNEL WITH POROUS BAFFLES", which he prepared after fulfilling the requirements specified in the associated legislations, before the jury whose signatures are below.

Thesis Advisor:	**Prof. Dr. Filiz BAYTAŞ** Istanbul Technical University	.....
Jury Members:	**Prof. Dr. Üner Çolak** Istanbul Technical University	.....
	Dr. Şule Kapkın Istanbul University	.....

Date of Submission : 20 September 2018
Date of Defense : 23 October 2018

ACKNOWLEDGEMENTS

In this study, a channel with porous baffles is designed and analysed in detail, in order to investigate the thermal energy transfer capability and the characteristics of the flow.
I, hereby, sincerely thank to my thesis supervisor Prof. Dr. Filiz Baytaş and my family for their incentive, support and help during the course of my research.

September 2018

Ahmet Baş
Mechanical Engineeer

TABLE OF CONTENTS

Page

ABBREVIATIONS

LTE	**:** Local thermal equilibrium
Nu	**:** Nusselt number
Pr	**:** Prandtl number
Re	**:** Reynolds number
REV	**:** Representative elementary volume

NOMENCLATURE

C	**:** Friction coefficient
C_E	**:** Ergun friction coefficient
c_p	**: S**pecific heat
f	**:** Friction factor
g	**:** Gravitational acceleration
K	**:** Permeability
k	**:** Turbulent kinetic energy
l	**:** Material thickness
p	**:** Average pressure
Q	**:** Flux
u_D	**:** Darcy velocity
V_p	**:** Pore space volume
V_s	**:** Solid volume
α	**:** Baffle inclination angle
α_{et}	**:** Effective thermal diffusion coefficient
ε	**:** Turbulent dissipation
ϕ	**:** Porosity
μ	**:** Fluid viscosity
ρ	**:** Fluid density
δ	**:** Baffle thickness

INDEX OF TABLES

Page

INDEX OF FIGURES

Page

GÖZENEKLİ ENGELLER BULUNAN BİR KANALDAKİ AKIŞIN SAYISAL OLARAK İNCELENMESİ

ÖZET

Gözenekli yapıya sahip malzemeler, insan hayatında diğer birçok farklı yapıdaki malzemeye nazaran daha eski bir geçmişe sahiptir. Günlük yaşantıda kullanılan mutfak süngerlerinden inşaat tuğlalarına, endüstriyel fırınlardaki seramiklerden konvansiyonel enerji dünyasının temel taşı olan kömürün yapısına dek birçok malzeme doğal olarak gözenekli yapıda bulunmakta veya insan etkisiyle bu hale getirilmektedir. Gözenekli yapıların incelenmesi ve endüstriyelleşmesi birkaç yüzyıl öncesine dayanmaktadır.

Bir yapısal malzeme özelliği olarak gözeneklilik, bundan yaklaşık iki yüz elli yıl kadar önce hidrolik ve akış alanlarında uzmanlaşmış bir Fransız mühendis olan Henri Darcy tarafından incelenmiştir. Darcy gözeneklilik ile birlikte geçirgenliğin de bu konuda dikkat edilmesi gereken bir diğer malzeme özelliği olduğunun farkına varmış ve yapmış olduğu deney ile akışın gözenekli ve geçirgen bir ortamdaki davranışını basınç düşümü ve akış dinamiği parametreleri ile açıklayan Darcy Yasası'nı ortaya koymuştur.

Darcy'nin gerçekleştirdiği çalışmaların ışığında, bilim insanları gözenekli yapıya sahip maddeler ile ilgili çalışmalarını günümüz problemlerine uyarlayarak enerji, otomotiv, inşaat gibi popüler sektörlerdeki problemler ile bu sektörlerin çevresel etkilerini iyileştirmeye yönelik konulara eğilmektedirler.

Bilimsel çalışmaların odağı, sektör veya dal farketmeksizin, her zaman daha fazla getiri elde etmek olmuştur. Hatta bunu bilimsel çalışma olarak kısıtlamak yerine tüm mühendislik çalışmaları olarak genellemek daha doğru olacaktır, zira mühendisliğin temelinde insan hayatı için ürün performansı, fiyatı, ağırlığı ve fonksiyonelliği açısından daima ileriye taşımak amaçlanmaktadır.

Termodinamik proseslerin en önemli aktörlerinden olan kullanılamayan ve açığa çıkan ısı veya bir diğer deyişle boşa giden iş, termodinamik alanındaki birçok çalışmanın ve bir bakıma bu çalışmanın da özünü oluşturmaktadır. Söz konusu çalışma, özetle, daha önce değinilen gözenekli malzemeler ile ısı transferi konularını yan yana getirerek bu konuda ortaya koyduğu hipotezi somut bulgularla kanıtlamayı amaçlamıştır.

Tez çalışmasına başlanırken, önerilen modelin güvenilir ve sağlıklı şekilde çalışıyor olduğunu göstermek amacı ile, daha önce yapılan çalışma modellerine benzetimler kurularak bu modellerden elde edilen sonuçlar ile karşılaştırılmıştır.

Benzetim yapılan ve literatürde yer alan çalışmada, gözenekli olmayan katı engeller çeşitli sayı, konum ve açılarda kanal içerisine yerleştirilerek, bu durumların yine akış karakteristiği ve bölgesel ısı transferine etkisi gözlemlenmiştir. Söz konusu model ayrıca kanalda oluşan hız profillerini de ele alarak, akışın gelişmiş akış veya

gelişmemiş akış olup olmadığını da incelemiştir. Türbülanslı akış rejimini sağlayacak Reynolds sayısı baz alınarak koşturulan analizlerde çözümleyici olarak literatürdeki benzer çalışmalarda olduğu gibi SIMPLE algoritmasından yararlanılmıştır.

Bu yüksek lisans tez çalışmasında, literatürdeki çalışmalar göz önüne alınarak içerinde gözenekli engellerin bulunduğu bir kanaldaki akış sayısal olarak incelenmiştir. Bu incelemeye başlamadan önce literatürde yer alan, kanal içerisinde katı engellerin bulunduğu bir makale ile çalışmanın doğrulanması gerçekleştirilmiştir.

Bu çalışmada, ele alınan modellerin sayısal olarak incelenmesinde literatür ile süreklilik ve karşılaştırma kolaylığı sağlaması açısından SIMPLE algoritması kullanılmış, analizler ise ANSYS Fluent modülünde gerçekleştirilmiştir.

Analizler iki boyutlu düzlemde gerçekleştirilmiştir. Arayüz olarak engeller ve akış arasında ağ ızgara üzerinden gözeneklilik kriteri tanımlanarak akış çözümleri birbirine bağlanmıştır. Kütle transferi, hız vektörleri, enerji ve türbülans karakterleri için yakınsama kriteri olarak alınan değer 10^{-5}'tir ve bahsi geçen değer, söz konusu incelemenin literatür araştırmasına konu olan diğer çalışmaların genelinde de yeterli görülmüştür.

Kanal uzunluğu 0.554 metre, kanal yüksekliği ise 0.146 metre seçilmiştir. Kanal içerisine yerleştirilen engellerin kalınlık değeri 0.01 m, boyları ise 0.1 metre alınmıştır. Engellerin eğiklik açıları olarak 45°, 60°, 90° açıları verilmiştir. Engellerin gözenekli olmasına istinaden gözeneklilik değerleri 0.4 ve 0.9 olarak değiştirilip, geçirgenlik için ise 10^{-9}, 10^{-8} ve 10^{-7} değerleri kullanılmıştır.

Akış rejimi olarak türbülanslı akış modelinin kullanılması öngörülmüştür. Bu amaçla Reynolds sayısı olarak 8.73×10^4 seçilmiştir. Korunum denklemleri de yine bu bağlamda gözetilerek ele alınmış ve çözüm modülünde ilgili değişiklikler yapılmıştır.

Ana sınıflandırma; gözenekli engellerin tekli, ikili ardışık ve ikili çapraşık olarak kanala konumlandırılması ile üç ana hal şeklinde yapılmıştır. Her bir hal, daha sonrasında, engellerin akışa karşı üç farklı açıda yerleştirilmesi ile düzenlenmiştir. Ardından, engellerin seçilmiş olduğu malzemenin çeşitli gözeneklilik ve geçirgenlik parametreleri değiştirilerek bu değişimlerin akış karakteristiğine ve bölgesel ısı transferine etkileri her bir hal için irdelenmiştir.

Sonuçlar incelendiğinde görüldüğü üzere ardışık veya çapraşık olarak yerleştirilmesi farketmeksizin ikincil bir gözenekli engelin kanala yerleştirilmesi, bölgesel ısı transferini artırmaktadır. Açısal olarak konumlandırılmalar değerlendirildiğinde ise bu kez sonuçların açı artışı ile birlikte iyileştiği görülmektedir. Bunun nedeninin, akış çizgilerindeki düzensizliğin ve buna bağlı olarak yeterli miktarda yeniden dolaşımın oluşması olduğu düşünülmektedir.

Bahsedilen sonuçlara ek olarak incelenen parametrelerden olan gözeneklilik açısından bakıldığında, gözeneklilik değişiminin sunulan hipoteze katkı sağlamadığı görülmektedir. Bir diğer parametre olan geçirgenlik değişiminde, beklenenin aksine yüksek geçirgenlikte yüksek hıza sahip olan akışkanın ısı transferinde düşüş gözlemlenmiştir. Buna sebep olarak akışkanın yeterli yeniden dolaşıma sahip olamadan kanalı terkederek engellerin yüzey alanlarından yararlanamayışı gösterilebilir.

Bu sonuçlar ışığında, gözenekli engellerin kanal içerisinde kullanımında dikkate alınacak unsurlardan engellerin sayısı, kanal duvarları ile yaptıkları açı, konumlandırılma şekilleri, kullanılan malzemenin gözeneklilik ve geçirgenlik değerleri için yapılacak seçimlerde göz önüne alınması gereken kriterler sunulmuştur. Ayrıca, kanaldaki akışa karşı duracak şekilde yerleştirilen engellerin açısının ve konumlandırılma türlerinin, engel sayısının ve malzemesinin gözeneklilik ve geçirgenlik parametrelerinin endüstriyel alandaki tasarımlara uygulanabilirliği için gereklilikler yorumlanmıştır.

NUMERICAL INVESTIGATION OF FLOW IN A CHANNEL WITH POROUS BAFFLES

SUMMARY

Porous materials have been used for more than many other materials types known to humans. From daily use such as bath or kitchen sponges to more general use like building bricks, one can see how common porous materials really are. Furthermore, industrialization of them started only a couple of hundred years from today.

It was first Henri Darcy, a French engineer specilized on hydraulics, who investigated the properties of porous materials such as porosity and permability. His work led many other scientists to focus on these properties and help the industrialization process. In recent years, investigations started to merge with modern world problems as in energy or automotive industries and related ecological problems.

In the aim of creating a sustainable structure for any industry in addition to aforementioned ones, one must look for higher efficiency. For higher efficiency, the next step to take is decreasing the number of entropy generators or actually reducing their effect as it is a fact that entropy always happens.

For this purpose, this work focuses on the one the major entropy generators, that is, unused or wasted heat by inspecting the streams of flow in a channel with the help of porous baffles put in front of the flow. Considering the local heat transfer amounts, it was aimed to find the best case of heat transfer by comparing different cases of baffle positions. Other works also conducted in similar models contribute the progress of this study, validation of the model proposed and evaluation of results.

As an initial step, a similar study of staggered and porous baffles was inspected. In said study; propagation of streamlines against baffles were inspected in terms of heat transfer and drag, for two fluids with different properties. In the second work, channel flow around solid baffles with different inclination angles was studied. Once the use of proposed model is confirmed, these two works were merged and analysed accordingly.

During analysis, the latter model was selected as the base model for grid, boundary conditions and flow regime; however, different cases were produced by crossing different porous medium properties for baffles. Moreover, categorization was based on number and placement of baffles in the channel as well as their angle of inclination.

After post-processing the analysis results, it was seen that the baffles that are positioned as staggered was the best case in terms of local Nusselt number and hence heat transfer capability as the baffle inclination angle was increased. On the other hand, contribution of porosity change was minimal to flow characteristics. Permeability effect was the opposite of expected, considering that the loss in flow speed would decrease convection heat transfer; however, the lower the permeability

the higher was the heat transfer values due to recirculation strength created around the baffles.

Eventually, in addition to above analytical results, an experimental research is always encouraged.

1. INTRODUCTION

Heat transfer and flow analyses in channels have always been attractive to researchers who are interested in fluid dynamics and energy branches. As the channel flow is being one of the basic type of flow studies, it had the chance to work as a baseline for many other studies and improvements such as investigation of channel flows with various specifications, obstacles etc. Not only for experimental or scientific researches, but also for several different industries such as chemical reactors, automotive or electronics where one can see a channel flow is employed; heat and flow efficiencies were drastically important. To be more specific, one can say that any industrial application using any type of simple heat exchanger will need to perform a deep dive for channel flow efficiency in order to increase the benefits gained from the whole process.

As a heat exchanger's construction can have different steps; turbulators or so-called baffles have always been a fundamental piece to increase the time and distance which fluid travels, hence providing more time and surface area for heat transfer. For example, in automotive industry, heat exchangers are responsible of cooling or heating different components at the same time and this requirement might require using different structures as shown in Figure 1.1 depending on the performance expectation.

Figure 1.1 : Different types of turbulators used in heat exchangers

Alignment of the technological improvements and the continuous search for efficiency increase in flow and thermal energies led the engineering world to investigate these aforementioned studies by combining heat exchanger structure with new material combinations. One of the most practical combinations of those was

definitely, which has also a great potential of being applied in industry, using porous material as the baseline of baffles in a channel flow with different flow regimes such as laminar or turbulent. Although the porous material is not very common in main industries, it is a great candidate for such applications where one needs the component sometimes to behave like solid and sometimes porous for specific occasions. It is certain that this beaviour can be defined by adjusting material specifications such as the amount of pores or the degree of permeability, which allows controlling the process in more detail with additional parameters.

1.1 Purpose of This Work

This work aims to study the characteristics of the around the different cases of porous baffles in a channel, with respect to a turbulent flow regime which assumes a simplified model of an intercooler of an automobile. Heat transfer analysis of the flow was performed for three main different conditions with several other subconditions. Nusselt number of the flow was calculated by evaluating the components such as heat flux, turbulence constants and velocity profile. Comparisons of the results to the similar models in the literature were performed and domain was inspected in detail. Computational grid, finite element method, geometrical cases and turbulence model that were evaluated in this work are based on the works of Louhibi et al. (2014). Moreover, material characteristics such as porosity and permeability data were referenced from Santos & de Lemos (2006).

1.2 Literature Review

Literature review conducted for this study includes the inspection of the general flow characteristics around a baffle in a channel flow, changes in these aforementioned characteristics once the baffle material is chosen to be as porous instead of solid and different cases of baffle placements into the channel in terms of number on positioning. Although there are similar studies in literature about porous baffles such as the works of Li et. al. (2010), Ko & Anand (2003) and Santos & de Lemos (2006); adding inclination angle to such baffles with porous material will also enable the applicability of this investigation to industry, especially to heat exchangers, since the versatility created by this proposal.

As an initiator in this area, Hwang (1997) has performed an experimental study where the staggered set of baffles were placed in front of a turbulent flowfield in a channel. He employed the SIMPLE algorithm to solve the flow characteristics and investigated the thermal performance and frictional losses; eventually found out that both were improved in terms of flow parameters.

In another work conducted by Yang & Hwang (2003) where air was selected as the working medium, design of a channel with staggered porous baffles arranged inside was made. Different baffle arrangements such as spacing or height were used in their study. After comparing the results to conventional solid baffles, it was confirmed that lower friction forces were seen in the channel with porous baffles.

Mahadevan et. al. (2013) studied a similar problem by investigating the pressure drop and heat transfer in a channel with low aspect ratio including carbon foams working as porous baffles. In their model, the effect of channel blockage on the heat transfer coefficient and pressure drop was observed. Their work concluded that although the heat transfer was high both in a channel with solid baffles and in a channel with porous baffles; however, porous baffles were created an advantage in terms of pressure drop.

In a more specific work, Li et. al. (2010) showed that the local heat transfer in a channel with porous blocks significantly enhanced with the increased thermal conductivity ratio between the fluid and the porous blocks.

Ko & Anand (2003) carried out a study by modeling a uniformly heated channel with porous baffles mounted on the walls. They also used staggered arrangement and selected different porous medium for baffles, as well as changing other parameters such as baffle thickness, hydraulic diameter and Reynolds number. At the end, they compared the results for heat transfer and pressure drop against the results of a straight channel with no baffles. Their results were proving a similar enhancement as in previous studies conducted by others.

In one of the recent works, Santos & de Lemos (2006) investigated the influence of porosity and permeability of the porous baffles on a laminar flow with different fluid properties. A channel with staggered baffles, and for those baffles different porosity properties were used. SIMPLE algotihm was employed as the numerical method. In their work, it was observed that the low porosity baffles have little effect on the flow

regime in terms of Nusselt number and friction factor, i.e. thermal energy and drag properties.

Yet another work using SIMPLE method by Louhibi et al. (2014) focuses on the effect of inclination of the baffles in a channel flow, claiming that increasing the baffle inclination angle would effect the heat transfer between channel walls positively. Hence, they designed a channel with different cases of baffle placements with 45°, 60° and 90° inclination angles. Their observation was proving their claims, however only for baffles made of solid material.

1.3 Hypothesis

The heat transfer properties and characteristics of a flow might be affected by different number of baffles placed with various inclination angles to a channel wall under turbulent flow regime. This problem can be investigated numerically.

2. THE FLOW IN POROUS MEDIA

A porous medium is defined as a whole of interconnected pores, which allows a fluid that is able to enter from one end and leave from the other. These pores can be found all over the material in different shapes and sizes. They can affect how the material will allow the fluid flowing through it or in other words, what kind of direction the fluid will follow.

When a fluid flows through a porous medium, there are two properties, which are called as porosity, and permeability and they need to be taken into account when employing governing equations for the flow. Saar & Manga (1999) explains porosity, ϕ, as a property that relates to how pore spaces are connected and how tortuous they are inside a material. In another words, porosity can also be described as the proportion of the pore space volume, V_p, to solid volume, V_s. This relation is given in Equation (2.1) below:

$$\phi = \frac{V_p}{V_p + V_s} \tag{2.1}$$

The permeability, K, represents a measure of the ability for flow through porous media and it can be written for a porous medium that consist of spherical particles as follow,

$$\mathrm{K} = \frac{\phi^3 d_p^2}{A(1-\phi)^2} \ (m^2) \tag{2.2}$$

where d_p is particle diameter, A is an experimental constant. This equation was obtained by experimentally by Ergün (1952).

As a pioneer in the area of flow through porous medium; Henri Darcy (1856), a French engineer, carried out an experiment which is related the flow through sand filters and observed the effect of permeability on pressure drop in terms of discharge velocity. His aim at first was to deliver clean water to a hospital building, however during many years, his work has gone through many reviews and updated by other

scientists who worked in the area of porous materials. In the experiment shown in Figure 2.1, Darcy created a test setup by using sand as a pack of porous material.

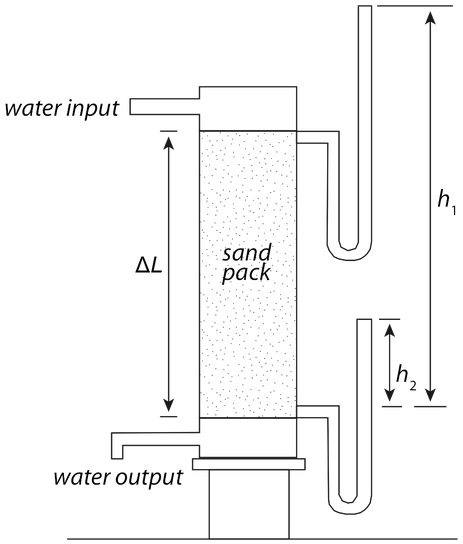

Figure 2.1 : Darcy's experiment setup described by Saar & Manga (1999).

The experiment was built on a vertical column, which has a water inlet at the top and outlet at the bottom. The water pressure in the system was controlled by the reservoirs. Darcy conducted series of tests with different packs of sand, measuring the change in pressure of inlet and outlet sections.

Darcy's law extracted out of this experiment is expressed in Equation (2.3) as:

$$p = -\frac{\mu}{K} u_D + \rho g \tag{2.3}$$

p = average pressure

ρ = fluid density

μ = fluid viscosity

g = gravitational acceleration

K = permeability of the porous medium

u_D = Darcy's velocity

From above equation, it can be noticed that the relationship between the pressure and velocity is linear and hence dependent of a proportionality constant. This would mean that the results should not change if Darcy would have used packs of another porous material. On the other hand, this equation is highly empirical, has a low flow

velocity and does not consider viscous effects. Hence, over the years, it has been improved and become more applicable to general cases of porous material investigations.

2.1 Area of Investigations For Porous Materials

After Darcy's breakthrough, porous materials have great attention from engineering world, especially from geology and related disciplines such as petrology or civil engineering and as well as energy sciences.

Ait-Mokhtar et al. (1999) studied the analytical and experimental modelling of porous medium together and chose to investigate granitic rocks' and cement mortars' porosity and permeability properties including the relationship between those.

In another study, Harpalani and Chen (1995) investigated how much effect pore matrix of coal would have on the methane gas outlet when the pore matrix changes.

A more recent work by Gaudillere and Serra (2016) touches both energy and automotive sectors by inspecting a fabrication method for highly porous ceramic supports as in Figure 2.2, with ordered pores to control the fluid transport, which would be used in fuel cells.

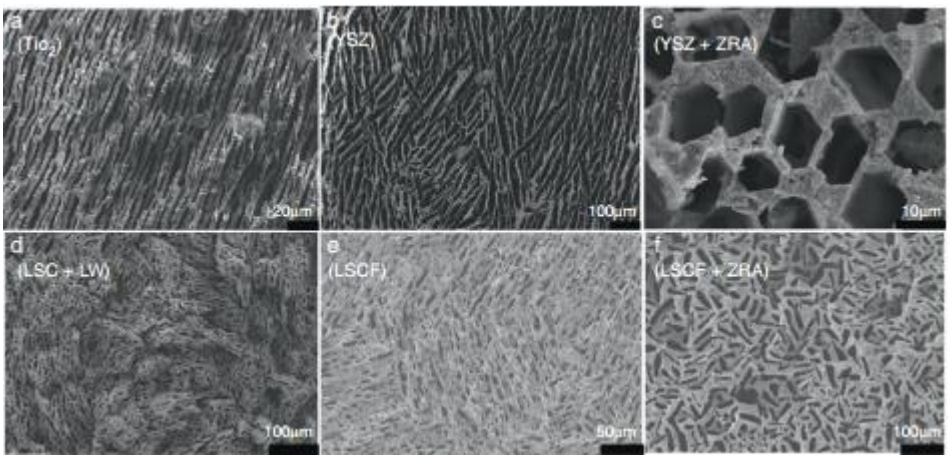

Figure 2.2 : Various fabricated porous ceramic materials from the work of Gaudillere and Serra (2016).

2.2 Types Of Porous Materials

Porous materials are widely common in nature or as well as can be man-made and considering that they can be found in several different types, shapes or properties;

there is a need for a categorization of them. Mainly, porous materials are classified according to their pore sizes.

Pore size is the most common property of a porous material when one would like to make a selection. Although it is becoming a research area for nanotechnology with the improvements in technology as in the work of Naik and Ghosh (2009), there are three major categories for pore size:

-Macroporous (>50 nanometers)

-Mesoporous (2-50 nanometers)

-Microporous (<2 nanometers)

As mentioned before, for nanotechnological purposes, they can be further subcategorized to supermicroporous, ultramicroporous, nanoporous and as such.

2.3 Governing Equations For Porous Media

In order to define the governing equations for porous medium, investigation in macroscopic scale is needed. For this reason, a representative elemantary volume (REV) is defined for the porous media composed of solid and fluid materials; so that it helps to classify the porous media as continous. REV is selected as in such size that it shows the same characteristics as the porous media. Although REV is a very small element when compared to whole system's size, it is still bigger than the pore size. Therefore; variables like temperature, velocity, density and pressure are represented with their volume averaged values.

2.3.1 Mass continuity equation

Mass continuity equation for flow in porous media is defined as below in Equation (2.4):

$$\phi \frac{\partial \langle \rho \rangle}{\partial t} + \nabla . \langle \rho \boldsymbol{v} \rangle = 0 \tag{2.4}$$

Here, ρ describes the fluid density and the brackets "$\langle\ \rangle$" show that the variable is volume averaged.

2.3.2 Volume averaged momentum equation

Navier-Stokes equation based on REV is given in Equation (2.5) by Vafai and Tien (1981) as follows:

$$\rho\left\{\frac{\partial\langle \boldsymbol{v}\rangle}{\partial t}+(\langle \boldsymbol{v}\rangle.\nabla)\langle \boldsymbol{v}\rangle\right\}=-\nabla\langle \boldsymbol{p}\rangle+\mu_e\nabla^2(\langle \boldsymbol{v}\rangle)-\frac{\mu}{k}\phi\langle \boldsymbol{v}\rangle- C\rho\phi^2|\langle \boldsymbol{v}\rangle|\langle \boldsymbol{v}\rangle+\rho\, g \tag{2.5}$$

In Equation (2.5); Baytaş (2006) defines the first term as the acceleration, the second term as the inertial terms, the third term as the change in pressure of the fluid flowing through porous media, the fourth term as viscous forces, the fifth term as Darcy flow effect and viscous friction force, the sixth and the seventh terms as form friction and body forces respectively. Equations (2.6) and (2.7) below describe the friction coefficient C.

$$C=\frac{C_E}{\sqrt{K}} \tag{2.6}$$

$$C_E=\frac{1.75}{(150\phi^3)^{1/2}} \tag{2.7}$$

Baytaş (2006) states that if the permeability of porous media, K, goes to infinity, the third and the fourth terms in Equation (2.5) becomes zero, hence it transforms to the Navier-Stokes equation which was written for the clear fluid.

2.3.3 Volume averaged energy equation

For a porous media which has an incompressible fluid flowing inside, volume averaged energy equation is given in Equation (2.8) by Baytaş (2006):

$$\rho_f c_{pf}\left\{\frac{\partial(\phi\langle T\rangle_f)}{\partial t}+\langle \boldsymbol{v}\rangle.\nabla\langle T\rangle_f\right\}=\nabla.\{k_f\nabla\phi\langle T\rangle_f\}+h(T_s-T_f)+\phi q_f{}''' \tag{2.8}$$

In the same manner, Equation (2.9) gives the volume averaged energy equation for the solid portion as:

$$(1-\phi)\left(\rho_s c_{ps}\right)\frac{\partial\langle T\rangle_s}{\partial t} = \nabla.\{k_s\nabla(1-\phi)\langle T\rangle_s\} + h\left(T_f - T_s\right) + (1-\phi){q_s}''' \tag{2.9}$$

In Equations (2.8) & (2.9), *s* and *f* subscripts indicate the solid and fluid phases of the porous media, where ${q_s}'''$ and ${q_f}'''$ describe the heat generation in solid and fluid phases themselves. In both equations, the second term in the right hand side models the heat transfer between two phases due to the fact that the solid and fluid temperatures are different in REV, that is, the phases are not in thermal equilibrium. Coefficient of convective heat transfer between the phases is defined by *h* and coefficients of conduction for solid and fluid are shown by k_s and k_f, respectively.

Thermal non-equilibrium approach expresses the temperature difference between the solid and fluid phases and in this case, the energy equation is solved separately for solid and fluid. On the other hand, if the temperature difference between the two phases is negligible, they are assumed to be in thermal equilibrium and a single equation is obtained like below Equation (2.10):

$$\sigma\frac{\partial\langle T\rangle}{\partial t} + \langle\boldsymbol{v}\rangle.\nabla\langle T\rangle = \nabla.\{\alpha_{et}\nabla\langle T\rangle\} + q''' \tag{2.10}$$

In above equation, σ describes the rate of heat storage capacity for the fluid saturated porous media, which is given in Equation (2.11):

$$\sigma = \frac{\varepsilon\left(\rho c_p\right)_a + (1-\varepsilon)(\rho c)_k}{(\rho c)_a} \tag{2.11}$$

Moreover, the effective thermal diffusion coefficient, $\boldsymbol{\alpha_{et}}$, is shown in Equation (2.12).

$$\alpha_{et} = \frac{\varepsilon k_a + (1-\varepsilon)k_k}{(\rho c)_a} \tag{2.12}$$

3. NUMERICAL ANALYSIS OF FLOW IN A CHANNEL WITH POROUS MATERIALS

In this study, it is investigated the change in the characteristics of a channel flow when different cases of porous baffles are placed into the channel with different angles, positioning and properties like porosity and permeability. These aforementioned properties and cases were applied into the analytical solver ANSYS – Fluent in order to solve the continuity, momentum and energy equations for porous medium and clear fluid in the channel.

For turbulent flow, k-ε model was employed and similar to previous ones, turbulence equations for turbulent kinetic energy and dissipation rate are solved by ANSYS – Fluent module. Turbulence model constants that were given in the next section are also entered into Fluent's solution module.

3.1 Macroscopic Equations

Equations have been used for the model given in Section 2.3. As a rule of thumb for every flow analysis, continuity and momentum equations were employed for the fluid. For continuity, Equation (2.4) was used for the incompressible fluid inside the porous media. Equation (2.5) was employed to solve the momentum of the flow. Since the temperature difference between the solid and the fluid was considered to be negligible, the system was assumed to be in thermal equilibrium; hence, Equation (2.10) was used to formulate local thermal equilibrium (LTE) along the channel. Calculation of local Nusselt numbers was contributed by each LTE solutions.

At last, turbulence flow regime characteristics were solved by turbulence kinetic energy and dissipation rate equations.

Turbulent kinetic energy, k and turbulent dissipation rate, ε are obtained from below Equation (3.1);

$$\frac{\partial}{\partial x}(\rho k u) = \frac{\partial}{\partial x}\left[\frac{\partial k}{\partial x}\left(\mu + \frac{\mu_t}{\sigma_k}\right)\right] + G_k + G_b + \rho\varepsilon \tag{3.1}$$

and Equation (3.2):

$$\frac{\partial}{\partial x}(\rho \varepsilon u) = \frac{\partial}{\partial x}\left[\frac{\partial \varepsilon}{\partial x}\left(\mu + \frac{\mu_t}{\sigma_\varepsilon}\right)\right] + C_{1\varepsilon}\frac{\varepsilon}{k}(G_k + C_{3\varepsilon}G_b) - C_{2\varepsilon}\rho\frac{\varepsilon^2}{k} \tag{3.2}$$

where $C_{1\varepsilon}$, $C_{2\varepsilon}$, $C_{3\varepsilon}$ are constants that are equal to 1.44, 1.92, 0.9; G_k, G_b are generation of turbulence kinetic energy due to velocity gradients and buoyancy, respectively. σ_k and σ_ε are turbulence Prandtl numbers for k and ε, which are defined as 1, 1.3. Furthermore, turbulent viscosity, μ_t, is calculated from below Equation (3.3) given by Santos & de Lemos (2006) where C_μ is constant and equal to 0.09:

$$\mu_t = \rho C_\mu \frac{k^2}{\varepsilon} \tag{3.3}$$

3.2 Mathematical Model

3.2.1 Geometric design

In this study, there are three cases for model geometry. The geometry, mesh grid and dimensions for Case 1 are shown in Figure 3.1 (a), 3.1 (b), respectively. However, for Case 2 and Case 3, first porous baffle's location is pulled ahead to L_i = 0.1 m and distance between two porous baffles is defined as 0.1 m again as seen in Figure 3.2 and 3.3. For these cases grid was kept same as Case 1.

A grid independence study was also conducted before starting the analysis. For this purpose, local Nusselt number values were selected for x = 0.45 m location of the channel and 90° inclination angle case. Five different grid options were analysed as seen in Table 3.1. After perfoming different runs, the most economical grid size was found to be 210x90 grid for the dimensions given in Table 3.2 and Table 3.3.

Table 3.1 : Grid independence study to compare local Nusselt numbers of presented study.

Grid-x	Grid-y	Nu	Time [min]
180	70	182.70	24
180	90	178.94	31
210	90	176.24	39
210	110	175.88	56
240	110	175.65	66

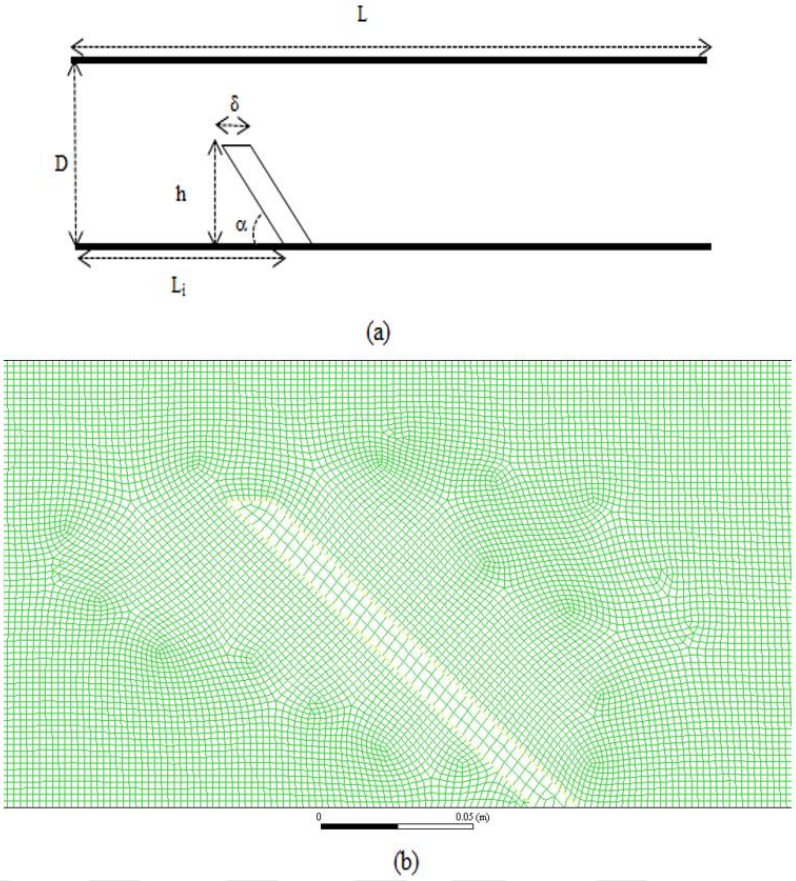

Figure 3.1 : Visual description of the channel (a) geometry and (b) mesh grid for Case 1.

Table 3.2 : Channel & baffle dimensions for Case 1.

L [mm]	h [mm]	D [mm]	L_i [mm]	δ [mm]
554	100	146	218	10

Other two cases are originated from Case 1 given above. The purpose investigating these two additional cases were to see the effect of baffle placement and number of baffles in front of the flow. Lastly, inclination angle changes are limited to three different angles for all cases.

In Figure 3.2 and 3.3 given below, it should be noted that L_i was changed to 0.1 m and an additional dimension between two baffles is defined as L_{ii}; which is set to 0.1 m.

Table 3.3 : Channel & baffle dimensions for Case 2 & Case 3.

L [mm]	h [mm]	D [mm]	L_i [mm]	δ [mm]	L_{ii} [mm]
554	100	146	100	10	100

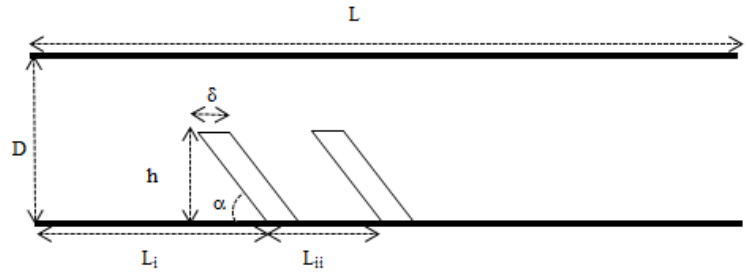

Figure 3.2 : Visual description of the channel for Case 2.

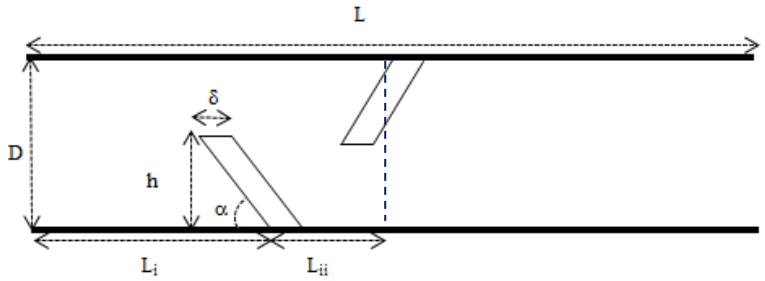

Figure 3.3 : Visual description of the channel for Case 3.

3.2.2 Boundary conditions

Boundary conditions are referenced from Louhibi et al. (2014) and given on the model in Figure 3.4. These boundary conditions are:

- inlet velocity in x-direction, u = 7.8 m/s
- inlet temperature, T_{in} = 300 K
- wall temperature, T_w = 373 K
- Reynolds number, Re = 8.73×10^4

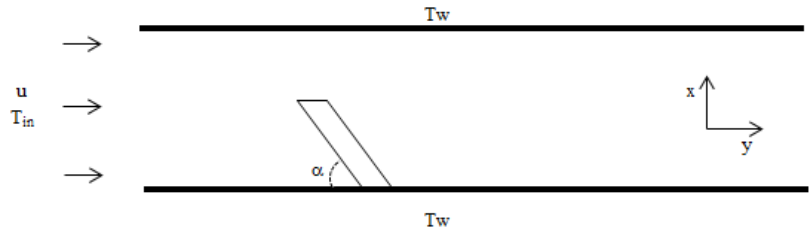

Figure 3.4 : Demonstration of the boundary conditions on the geometric model.

3.3 Numerical Method

Calculation of the flow field in the channel is performed by applying SIMPLE (Semi-Implicit Method for Pressure-Linked Equations) algorithm proposed by

Patankar (1980). This algorithm was integrated into ANSYS – Fluent's solution module along with many other solution algorithms. This module is able to perform algorithm runs via either Green-Gauss cell based or Least Square cell based discretization methods under density or pressure based coupling operations. For this study, pressure based operation and Least Square cell based discretization method was selected to solve SIMPLE algorithm.

Algorithm operates in the order below;

- making a guess for pressure,
- solving momentum equations for velocity,
- correcting pressure value,
- finding the other unknowns (temperature, turbulence parameters) using the corrected pressure,
- treating the corrected pressure as a new guess,
- re-iterating.

Convergence rate of the algorithm depends on the initial guess and other parameters defined by boundary conditions.

For the solution convergence, all convergence limits are selected as 10^{-5} for velocity, momentum and energy variables. Equations are solved per Second Order Upwind method.

3.4 Validation of the Study

There are different studies in literature that investigates the ways of improving flow characteristics in a channel as described in the previous section. The study of Louhibi et al. (2014) is focused on the investigation of a flow field around solid baffles in a channel with different inclination angles to flow direction and their study was selected for the validation of this study. Under turbulent flow regime; by SIMPLE algorithm, thermal and streamline behaviors of air was analyzed.

It must be noted that Louhibi et al. (2014) created a code to analyze and predict the thermal and dynamic behavior of their study for the solid baffles. On the other hand,

for the validation of this portion of the thesis, flow against the solid baffles was analyzed completely by ANSYS – Fluent's embedded SIMPLE algorithm.

Only a single Reynolds number value was taken into account which was chosen as $Re = 8.73 \times 10^4$ and this value was referenced to a velocity of 7.8 m/s in x-direction. k-ε model was employed as the baseline of the turbulent flow in Louhibi et al. (2014). Geometry for their study is same as Case 1 in our study; however, the baffles are selected as solid material.

Three different cases were investigated which are based on three different baffle inclination angle $\alpha = 45°, 60°, 90°$ and the Nusselt number for all these three cases was calculated within 0.05 m steps between the inlet and the outlet of the channel.

Analyses of a single baffle, which behaves like a cooling turbulator in a heat exchanger, with different inclination angles generated below streamlines and temperature contours along the channel as visualized in Figure 3.5 and Figure 3.6 for Louhibi et al. (2014) and presented study. As it can be seen from the Figures 3.5 and 3.6, the streamlines and temperature contours are similar for both studies.

In Figure 3.7 (a) and 3.7 (b); it was shown a comparison for the local Nusselt number, the values of Nusselt number of Louhibi et al. (2014) and those of presented study are found very similar.

Velocity profiles of different cases taken at 0.45 m line of the channel are considerably close to each other as given in Figure 3.8 (a) and 3.8 (b).

Temperature profiles which are shared in Figures 3.9 (a) and 3.9 (b) match with the literature work except a negligible disruption in 60° case.

Finally, one can say that these results indicate that in terms of flow characteristics, proposed model aligns well with the literature work. In addition, for each angle of baffle inclination, local Nusselt numbers of both original study by Louhibi et al. (2014) and presented study are very close to each other numerically.

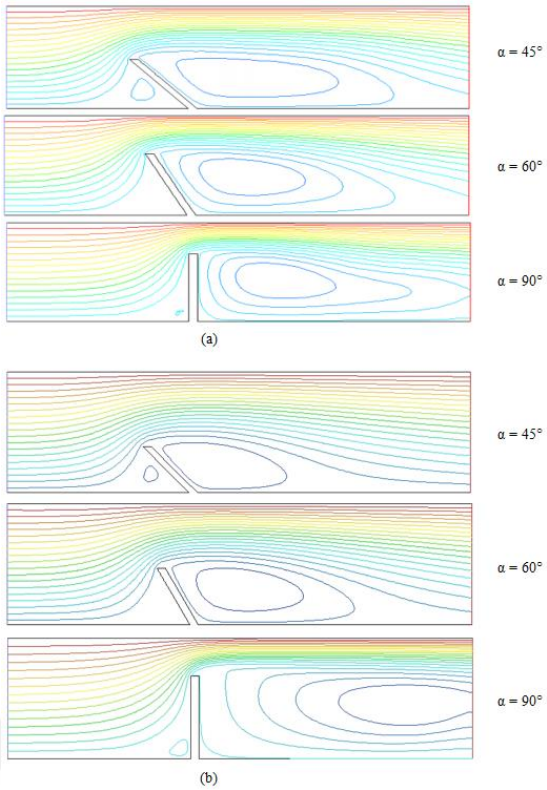

Figure 3.5 : Comparison of streamlines for flow against solid baffles (a) from Louhibi et al. (2014) and (b) from presented study with various inclination angles.

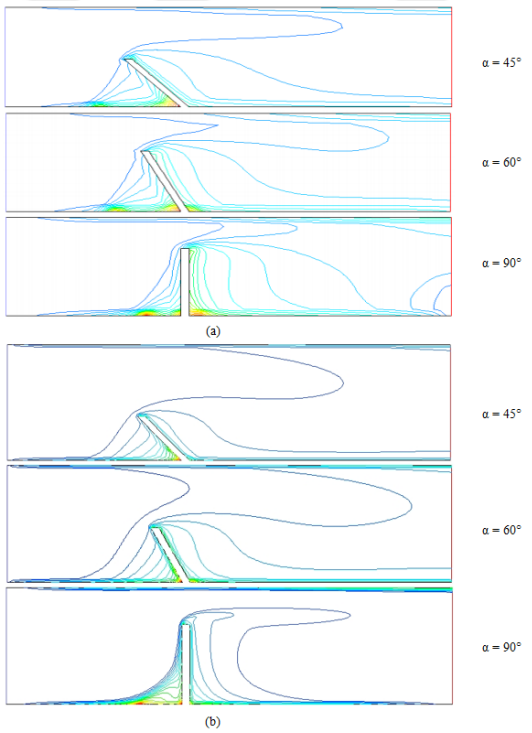

Figure 3.6 : Comparison of temperature contours for flow against solid baffles (a) from Louhibi et al. (2014) and (b) from presented study with various inclination angles.

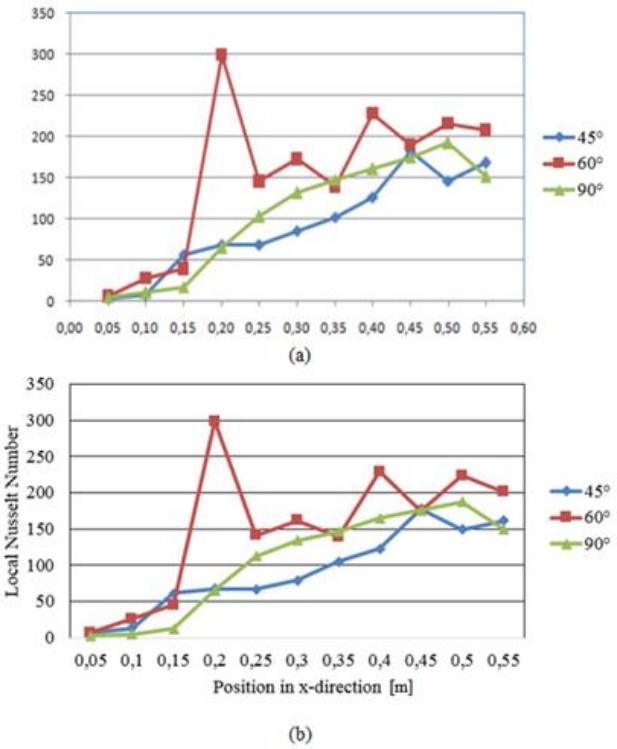

Figure 3.7 : Comparison of change in local Nusselt number in the channel per inclination angle, for solid baffles (a) from Louhibi et al. (2014) and (b) from presented study.

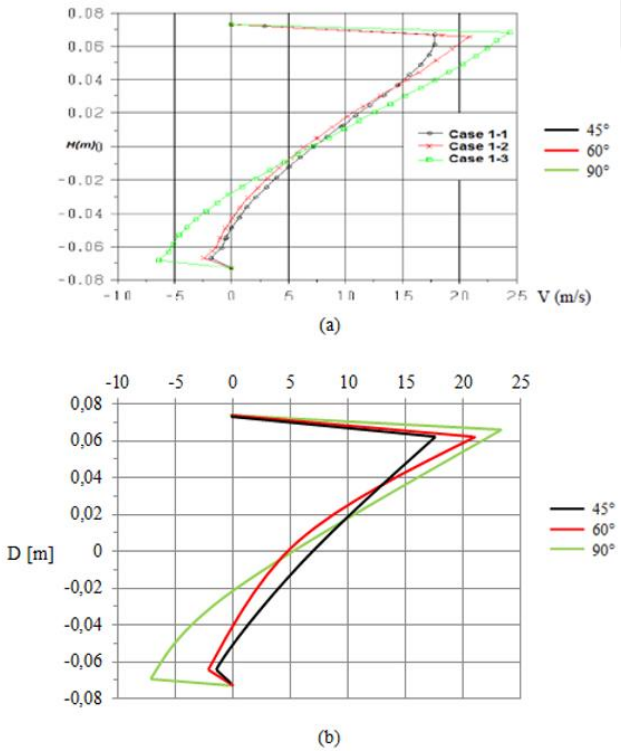

Figure 3.8 : Comparison of velocity profiles taken at x = 0.45 in the channel per each inclination angle, for solid baffles (a) from Louhibi et al. (2014) and (b) presented study.

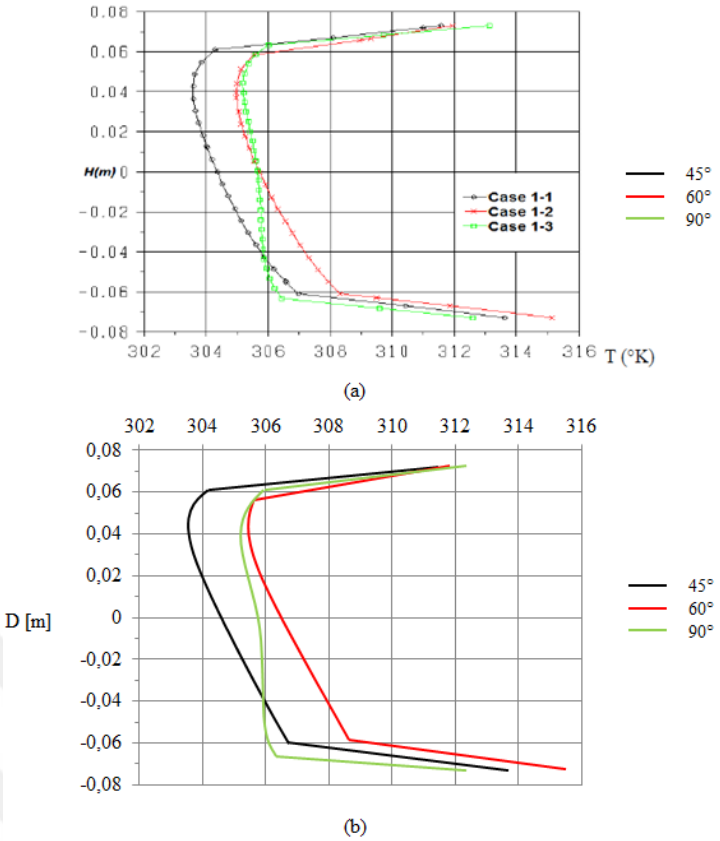

Figure 3.9 : Comparison of temperature profiles taken at x = 0.45 in the channel per each inclination angle, for solid baffles (a) from Louhibi et al. (2014) and (b) presented study.

3.5 Investigation Of Flow In A Channel With Porous Baffles

As described in the details of the model, results are divided into three main categories based on the number and positioning of the baffles as well as subcategories per inclination angles. Furthermore, an additional case is studied considering what would be the difference between porous and solid baffles.

3.5.1 Case 1

In this case, a single baffle is placed into the channel considering the given boundary conditions. Inclination angles of the baffle are taken as 45°, 60°, 90° respectively. For all cases, the effect of permeability as $K = 1 \times 10^{-9}$ m^2, $K = 1 \times 10^{-8}$ m^2, $K = 1 \times 10^{-7}$ m^2 and the values of porosity as $\phi = 0.4$, $\phi = 0.9$ are inspected in detail. In Figure 3.10 and Figure 3.11, distribution of streamlines and temperature contours along the channel are shown for different inclination angles, $K = 1 \times 10^{-9}$ m^2 and $\phi = 0.4$.

As seen Figure 3.10 and 3.11, there is more disturbance to flow while the inclination angle increases. Therefore, only in the case of 90° baffle angle, flow has a chance to get closer to the baffle when it is more develeoped and keeps its velocity. Advantage of this can be seen in Figure 3.12, as a reflection of local Nusselt number, hence as the heat transfer. Figure 3.13 shows the velocity profile observed at x = 0.45 m line of the channel. One can see that the velocity vectors do not turn to negative direction unlike solid baffle case given in previous section, if the baffle material is porous. Temperature profiles for different inclination angles in Figure 3.14 explains that when the porous baffles are used, there is more temperature difference due sharper velocity profiles.

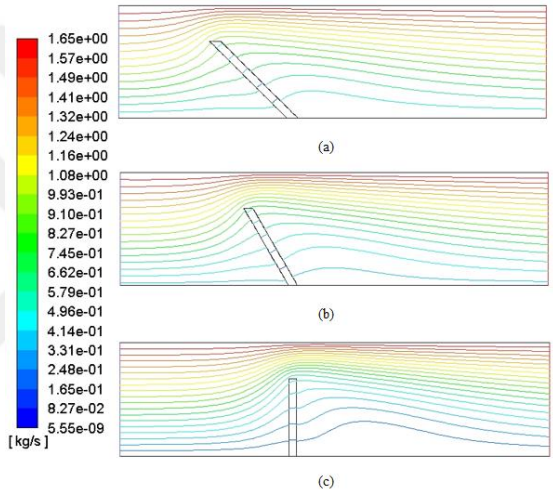

Figure 3.10 : Streamlines for a porous baffle in channel with three different inclination angles; (a) 45°, (b) 60°, (c) 90°.

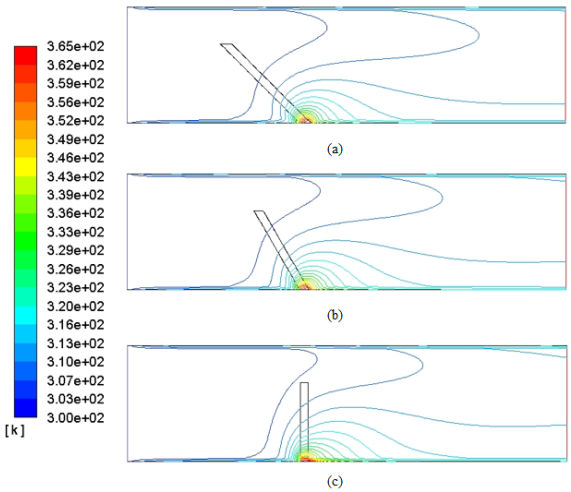

Figure 3.11 : Temperature contours for a porous baffle in channel with three different inclination angles; (a) 45°, (b) 60°, (c) 90°.

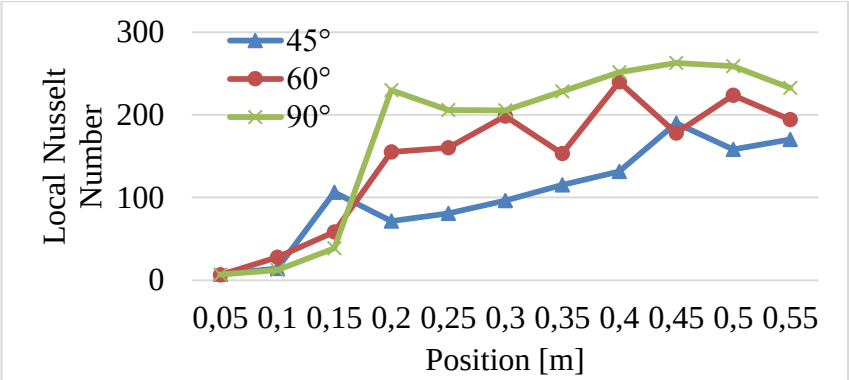

Figure 3.12 : Effect of baffle inclination angle on local Nusselt Number.

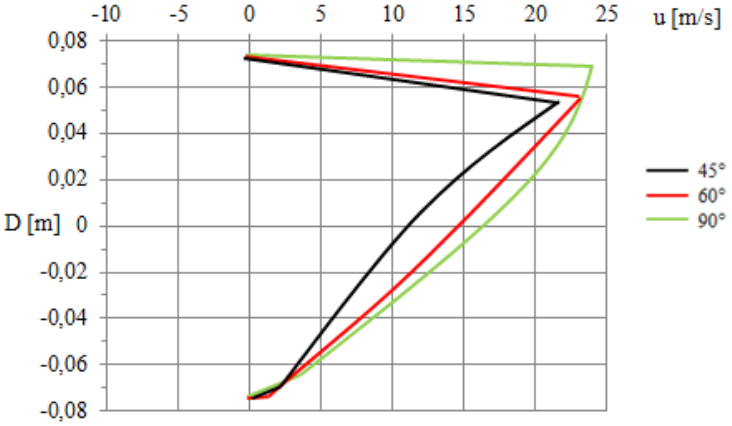

Figure 3.13 : Velocity profile for a baffle in channel at x = 0.45 m with three different inclination angles; 45°, 60°, 90°.

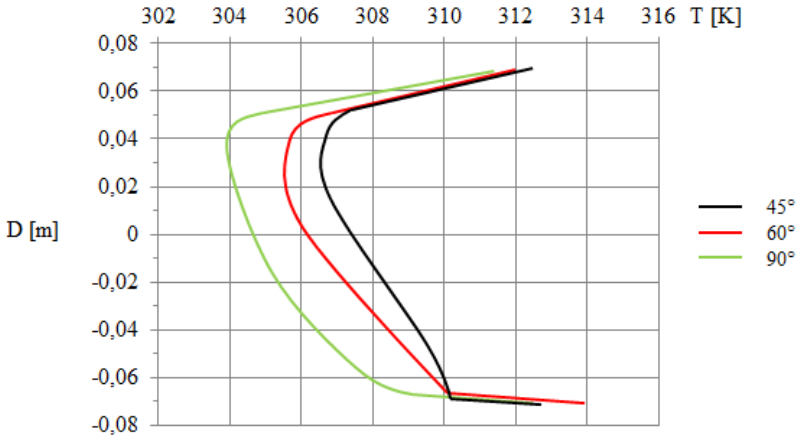

Figure 3.14 : Temperature profile for a baffle in channel at x = 0.45 m with three different inclination angles; 45°, 60°, 90°.

3.5.1.1 Effect of porosity change

Porosity value of porous baffle is changed as 0.4 and 0.9, in order to see the effect of porosity change in the case of baffle inclination angle is kept as 90°. As Figures 3.15,

3.16 and 3.17 shows, the porosity change has almost no effect on either streamlines, temperature contours and local Nusselt number.

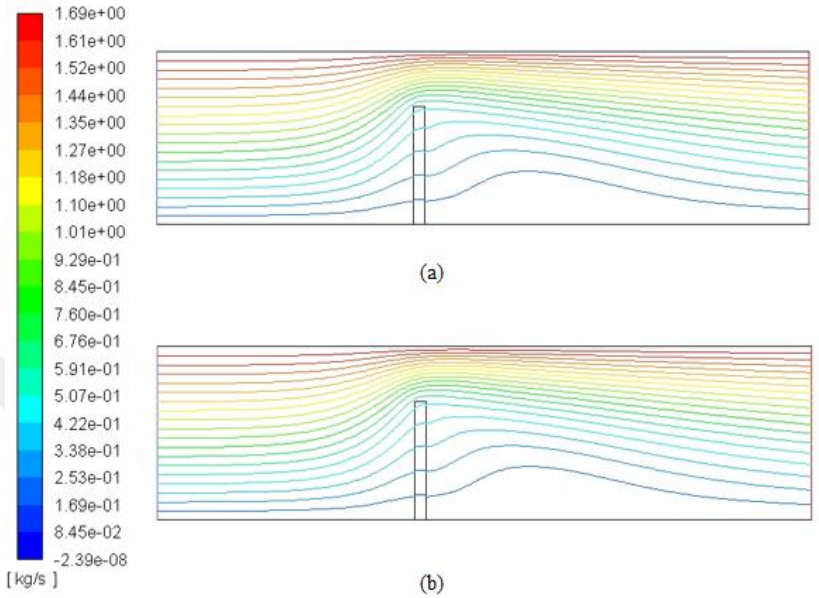

Figure 3.15 : Streamlines for a baffle in channel with porosity values (a) 0.4 and (b) 0.9, respectively.

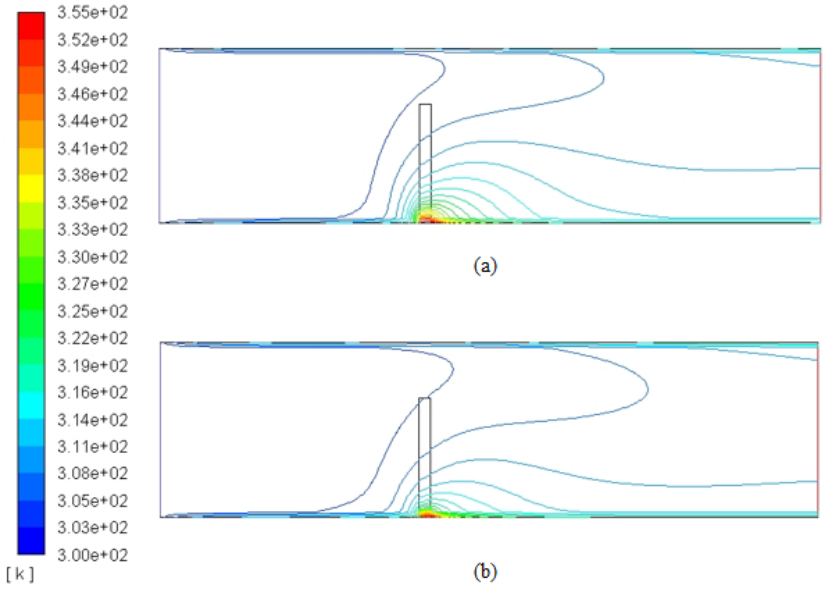

Figure 3.16 : Temperature contours for a baffle in channel with porosity values (a) 0.4 and (b) 0.9, respectively.

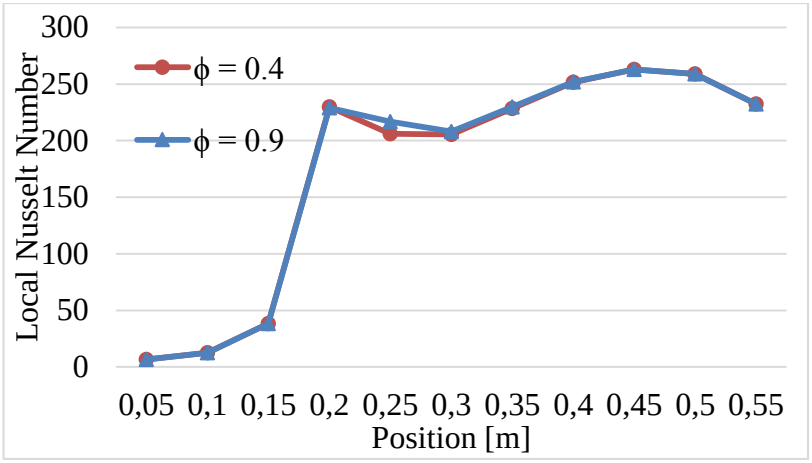

Figure 3.17 : Effect of baffle porosity on local Nusselt Number for a baffle in channel with 90° inclination angle.

3.5.1.2 Effect of permeability change

The effect of permeability of the porous baffle was also investigated for 90° inclination angle and porosity ϕ =0.4. In Figures 3.18, 3.19 and 3.20, one can see that as the permeability increases, therefore flow is less and less disturbed by baffle, heat transfer reduces as well. Although there is little difference between $K = 1 \times 10^{-8}$ m^2 and $K = 1 \times 10^{-7}$ m^2, there is a great contribution to heat transfer in the wake region after the baffle when the permeability is reduced to $K = 1 \times 10^{-9}$ m^2. Similarly, flow can move more easily with increasing permeability as shown in Figure 3.21. On the contrary, in Figure 3.22, temperature profiles grow in reverse direction of velocity. However, temperature difference remains similar to before due to heated wall condition.

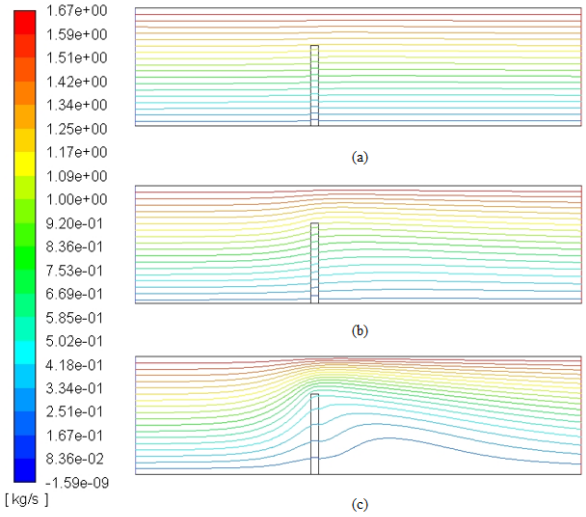

Figure 3.18 : Streamlines for a baffle in channel with permeability values (a) $K = 1 \times 10^{-7}$ m^2, (b) $K = 1 \times 10^{-8}$ m^2, (c) $K = 1 \times 10^{-9}$ m^2, respectively.

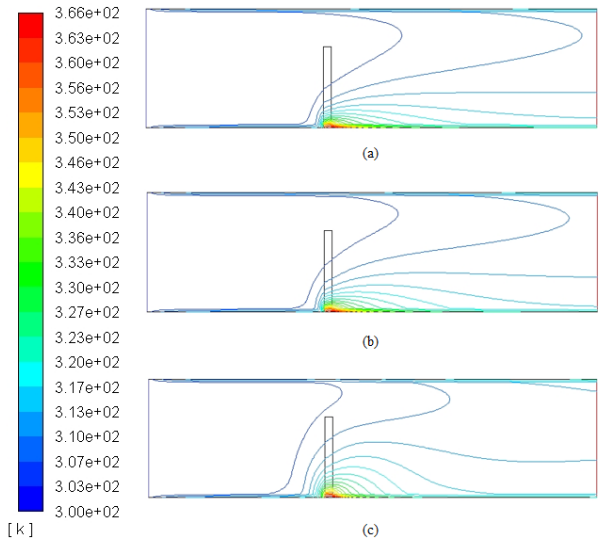

Figure 3.19 : Temperature contours for a baffle in channel with permeability values a) K = 1 × 10^{-7} m^2, (b) K = 1 × 10^{-8} m^2, (c) K = 1 × 10^{-9} m^2, respectively.

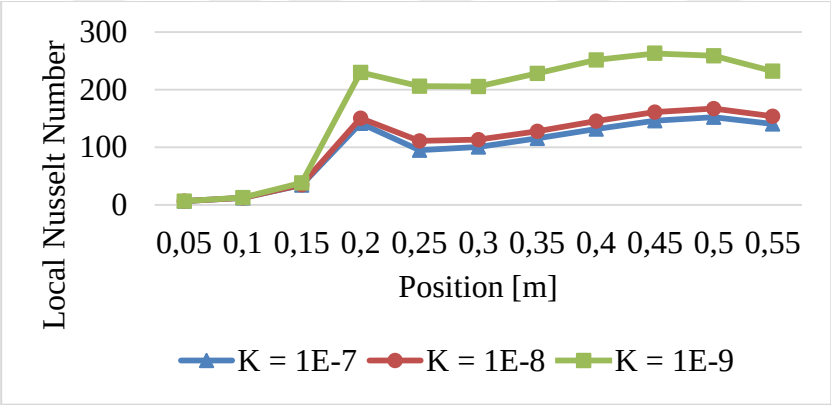

Figure 3.20 : Effect of baffle permeability on local Nusselt Number for a baffle in channel with 90° inclination angle.

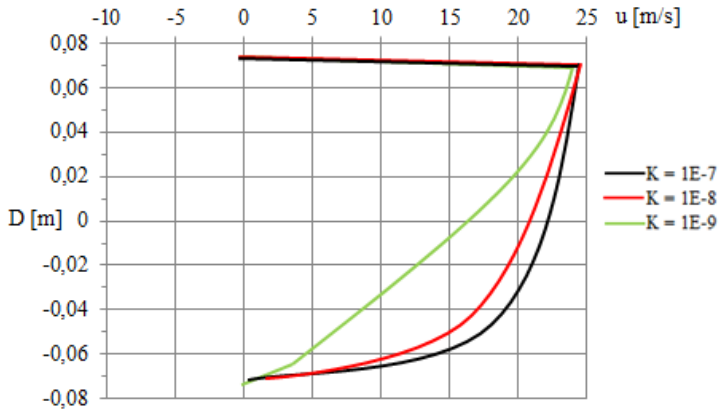

Figure 3.21 : Effect of baffle permeability on velocity profile for a baffle in channel with 90° inclination angle.

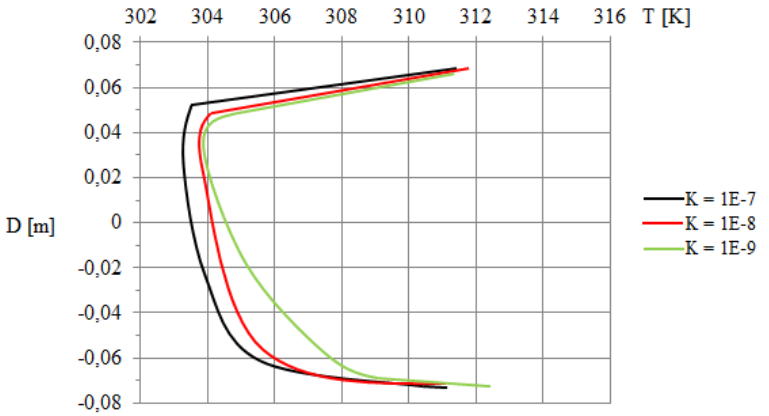

Figure 3.22 : Effect of baffle permeability on temperature profile for a baffle in channel with 90° inclination angle.

3.5.2 Case 2

In Case 2, two baffles are placed into the channel in tandem, again considering the given boundary conditions. Baffle inclination angles are not changed and kept as 45°, 60°, 90° respectively. Permeability values are chosen as $K = 1 \times 10^{-9}$ m^2, $K = 1 \times 10^{-8}$ m^2, $K = 1 \times 10^{-7}$ m^2 and porosity as $\phi = 0.4$ and $\phi = 0.9$. In Figure 3.23 and Figure 3.24, distribution of streamlines and temperature contours along the channel are given for three different inclination angles, $K = 1 \times 10^{-9}$ m^2 and $\phi = 0.4$.

When the baffle inclination angle is taken as 45°, flow is almost immediately distracted; however, this distraction is more evenly distributed to the area between the baffles and to the wake region. On the contrary, in 90° case, most of the eddies are accumulated after the second baffle. Figure 3.25 shows that the worst case is where inclination angle is the smallest. As the angle increases, average heat transfer value also increases similar to what was found in Case 1. Figure 3.26 and Figure 3.27 shows how this type of positioning of two baffles affects the velocity and temperature profiles in the channel.

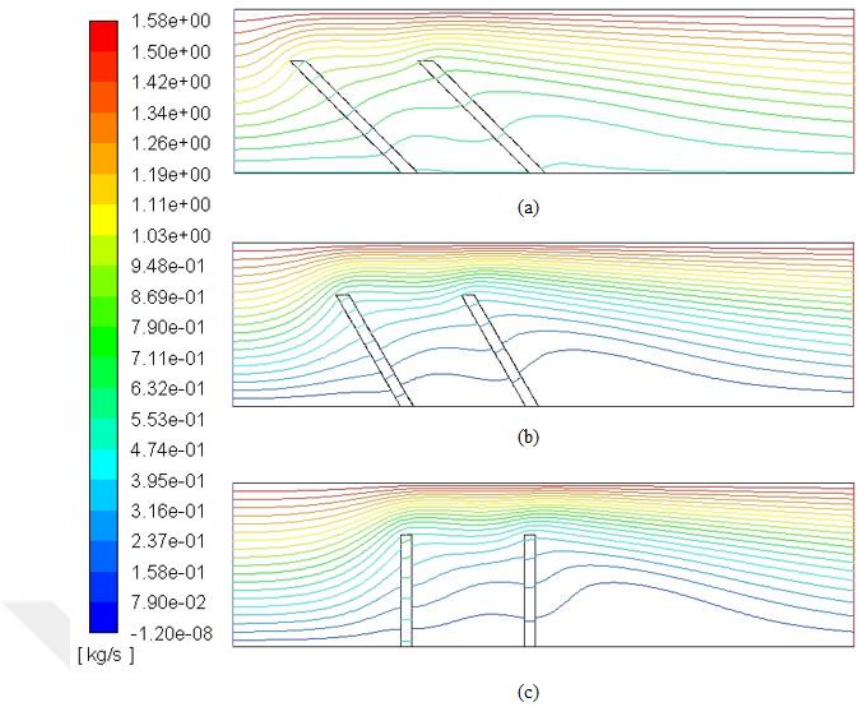

Figure 3.23 : Streamlines for two porous baffles as tandem in channel with three different inclination angles; (a) 45°, (b) 60°, (c) 90°.

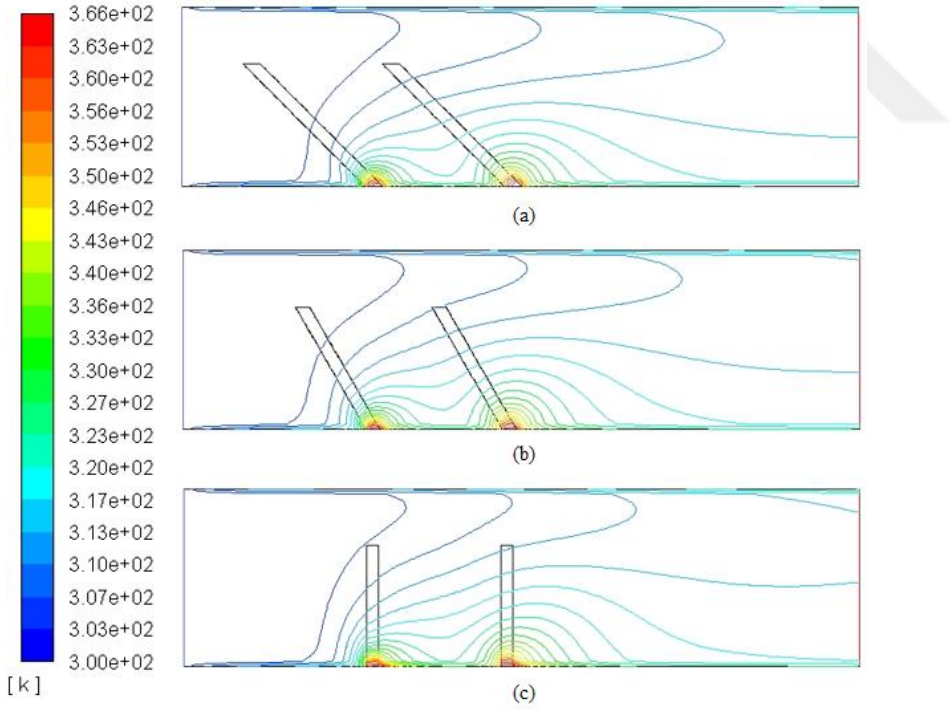

Figure 3.24 : Temperature contours for two porous baffles as tandem in channel with three different inclination angles; (a) 45°, (b) 60°, (c) 90°.

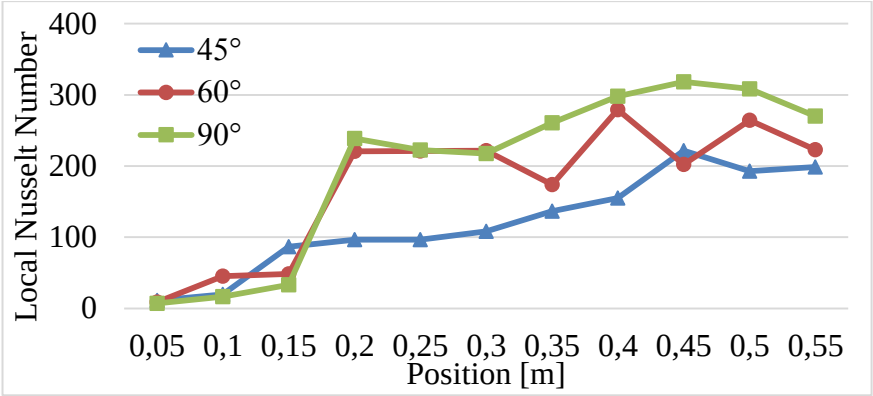

Figure 3.25 : Effect of baffle inclination angle on local Nusselt Number.

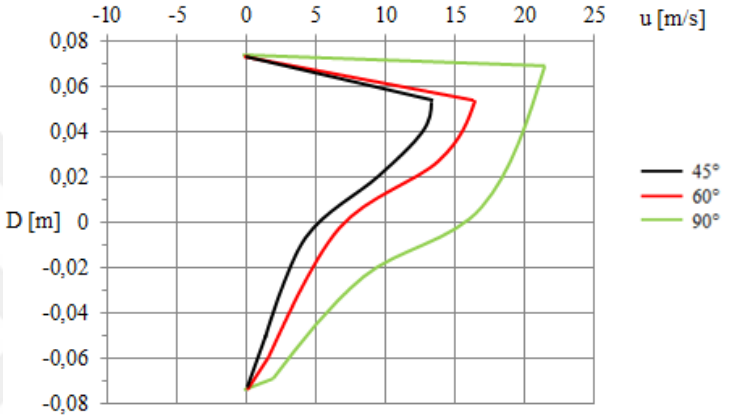

Figure 3.26 : Velocity profiles at x = 0.45 m for two baffles as tandem in channel with three different inclination angles; 45°, 60°, 90°.

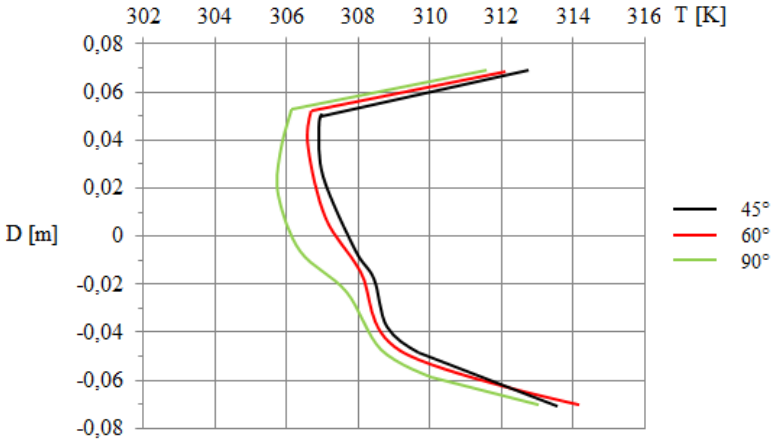

Figure 3.27 : Temperature profiles at x = 0.45 m for two baffles as tandem in channel with three different inclination angles; 45°, 60°, 90°.

3.5.2.1 Effect of porosity change

Similar to Case 1, porosity value is switched between 0.4 and 0.9, and visualised in Figures 3.28, 3.29. Furthermore, in Figure 3.30 it is shown that this change has little

effect on local Nusselt number. Like before, only 90° tandem structure is taken into consideration. No effect is seen by porosity change.

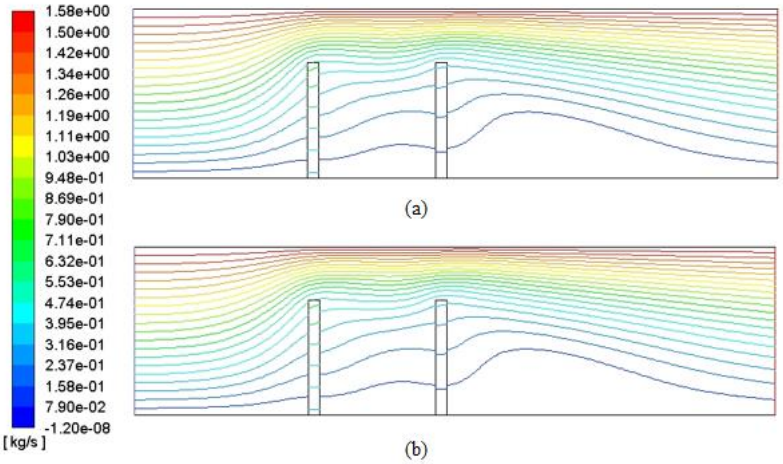

Figure 3.28 : Streamlines for two baffles as tandem in channel with porosity values (a) 0.4 and (b) 0.9, respectively.

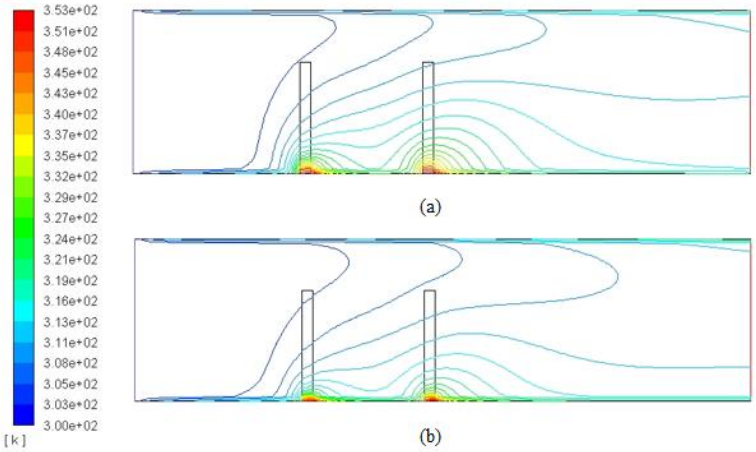

Figure 3.29 : Temperature contours for two baffles as tandem in channel with porosity values (a) 0.4 and (b) 0.9, respectively.

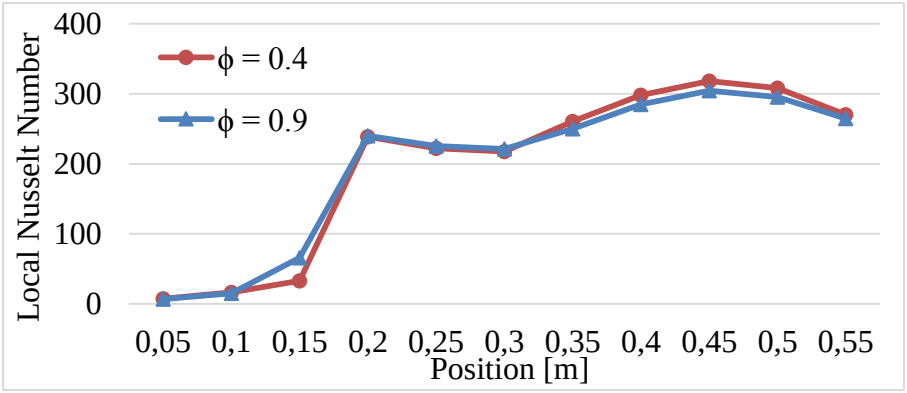

Figure 3.30 : Effect of baffle porosity on local Nusselt Number for two baffles as tandem in channel with 90° inclination angle.

3.5.2.2 Effect of permeability change

Again similar to what was done in Case 1, permeability is studied for Case 2 as in three different values which are $K = 1 \times 10^{-9}$ m^2, $K = 1 \times 10^{-8}$ m^2, $K = 1 \times 10^{-7}$ m^2. Figures 3.31, 3.32 and especially Figure 3.33 show the permeability's effect on heat transfer as to what was discovered in Case 1. The less the permeability, the more the contribution to local heat transfer is found. There is one difference from Case 1 though, it can be said that the average heat transfer in tandem case is higher than that of Case 1 where a single baffle is used. Figure 3.34 and Figure 3.35, on the other hand, prove that the permeability becomes a dominant material characteristic on velocity and temperature profiles.

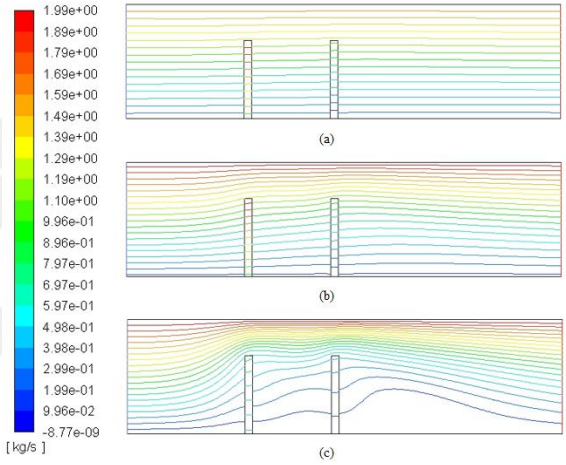

Figure 3.31 : Streamlines for two baffles as tandem in channel with permeability values (a) $K = 1 \times 10^{-7}$ m^2, (b) $K = 1 \times 10^{-8}$ m^2, (c) $K = 1 \times 10^{-9}$ m^2, respectively.

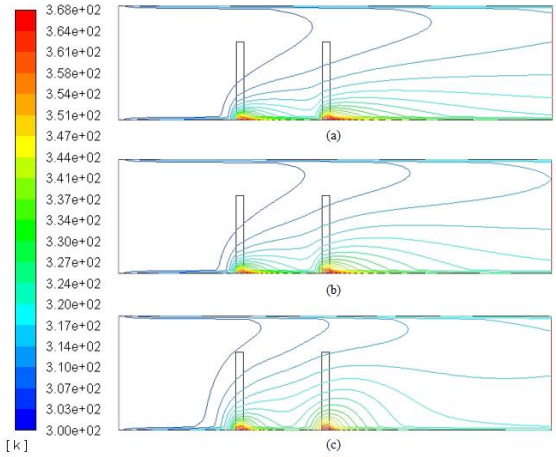

Figure 3.32 : Temperature contours for two baffles as tandem in channel with permeability values (a) $K = 1 \times 10^{-7}$ m^2, (b) $K = 1 \times 10^{-8}$ m^2, (c) $K = 1 \times 10^{-9}$ m^2, respectively.

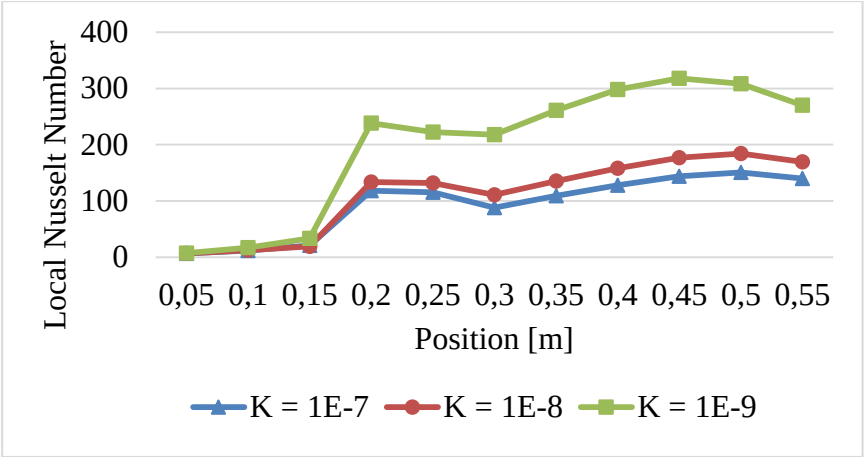

Figure 3.33 : Effect of baffle permeability on local Nusselt Number for two baffles as tandem in channel with 90° inclination angle.

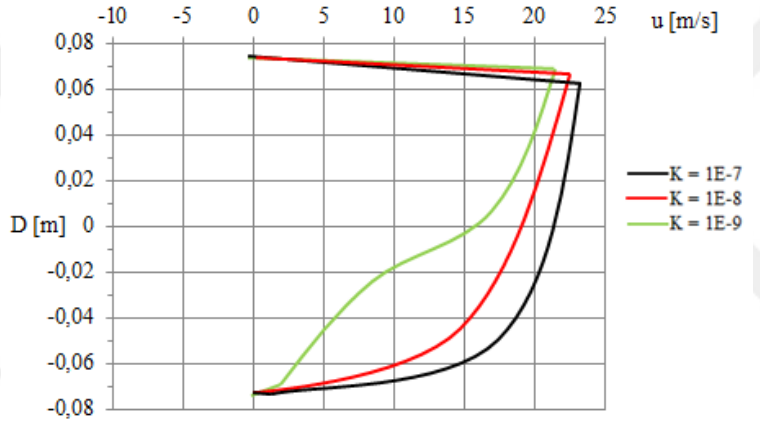

Figure 3.34 : Effect of baffle permeability on velocity profile for two baffles as tandem in channel with 90° inclination angle.

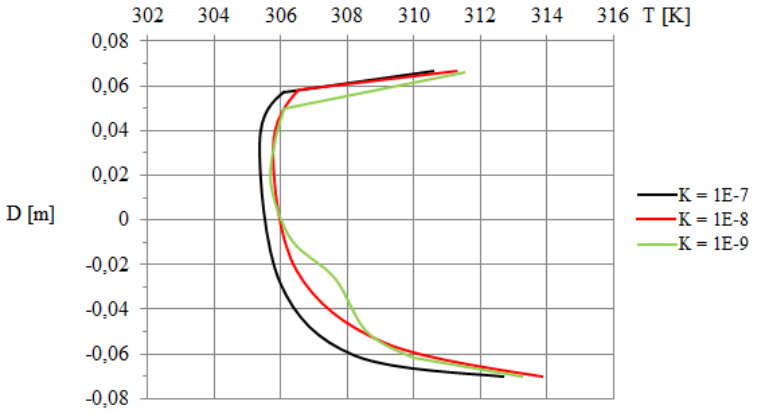

Figure 3.35 : Effect of baffle permeability on temperature profile for two baffles as tandem in channel with 90° inclination angle.

3.5.3 Case 3

Using the same boundary conditions provided for Case 1 and Case 2; in Case 3, two baffles are placed as staggered and the behavior of streamlines and local Nusselt number is investigated. Inclination angle of the baffles are not changed, that is, kept as 45°, 60°, 90° respectively. Likewise, permeability is kept as $K = 1 \times 10^{-9}$ m^2, $K = 1 \times 10^{-8}$ m^2, $K = 1 \times 10^{-7}$ m^2 and porosity as $\phi = 0.4$, $\phi = 0.9$.

Disturbance in streamlines and distribution of thermal contours can be seen in Figure 3.36 and Figure 3.37. If one looks at the local Nusselt numbers in Figure 3.38, it is obvious that staggered baffles with 45° gives the worst values of all three cases of baffle placements and inclination angles. This effect can also be explained by the velocity profiles from Figure 3.39 and temperature profiles from Figure 3.40. Although the velocity vector direction never becomes negative as in the case of solid baffles, flow is seriously slowed down due to the placement of baffles. As for the temperature values, it can be seen that the range between upper and lower limits reduced and became closer to each other.

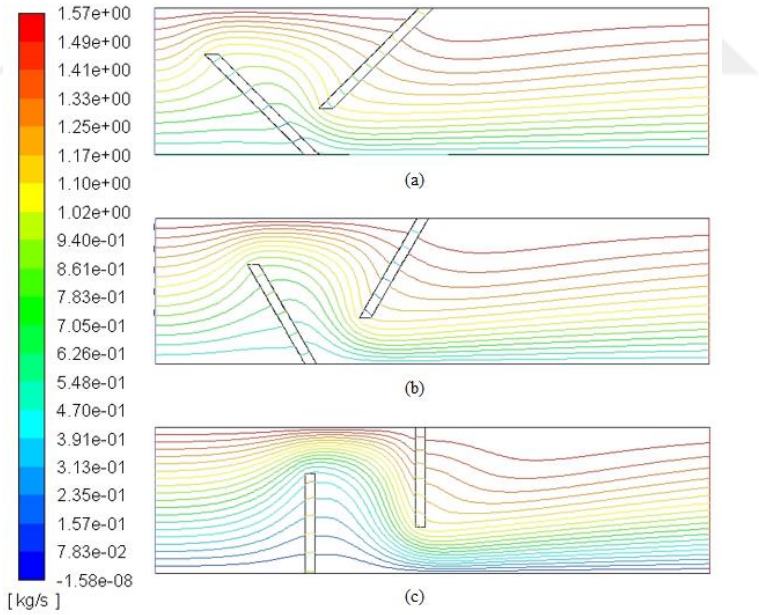

Figure 3.36 : Streamlines for two staggered baffles in channel with three different inclination angles; (a) 45°, (b) 60°, (c) 90°.

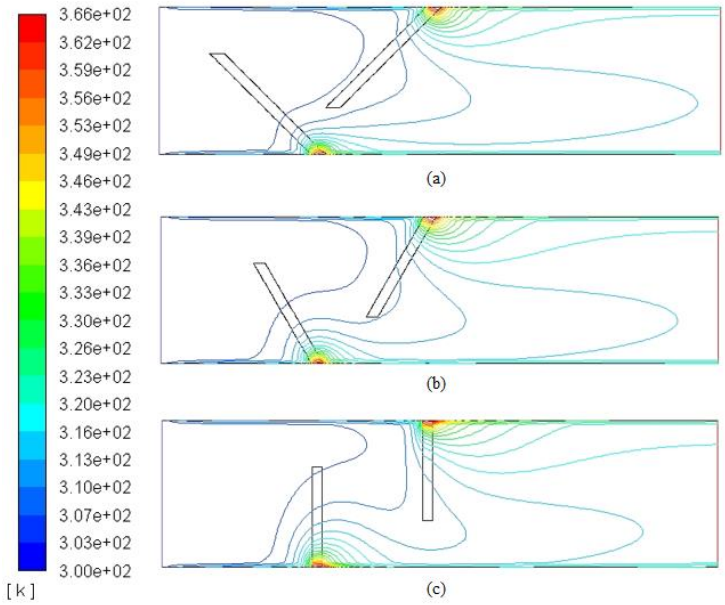

Figure 3.37 : Temperature contours for two staggered baffles in channel with three different inclination angles; (a) 45°, (b) 60°, (c) 90°.

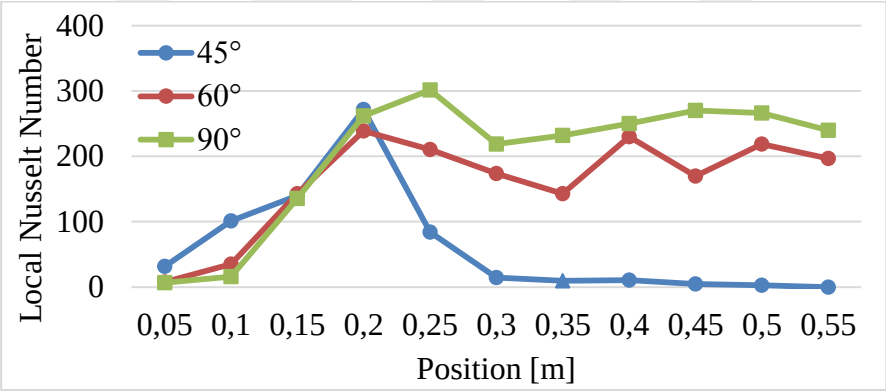

Figure 3.38 : Effect of baffle inclination angle on local Nusselt Number.

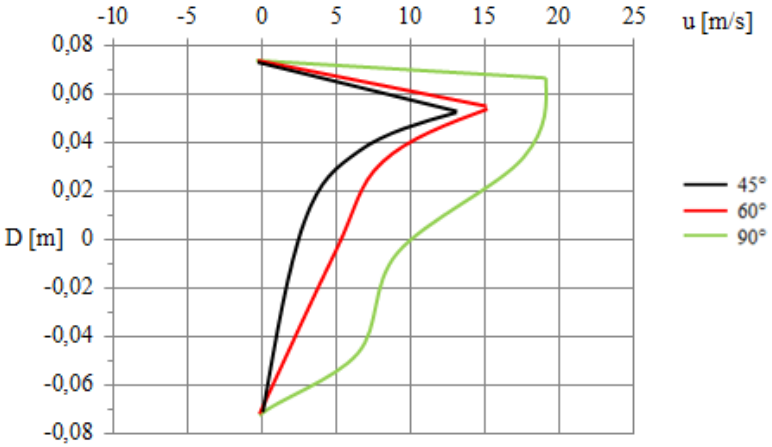

Figure 3.39 : Velocity profiles at x = 0.45 m for two staggered baffles in channel with three different inclination angles; 45°, 60°, 90°.

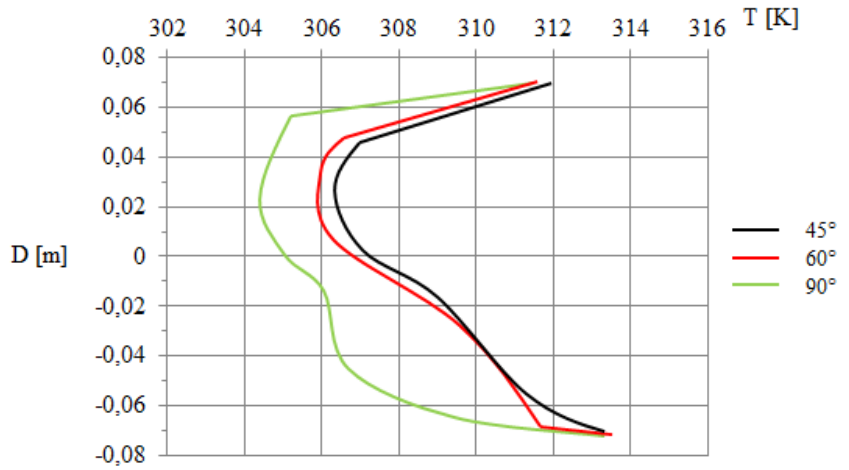

Figure 3.40 : Temperature profiles at x = 0.45 m for two staggered baffles in channel with three different inclination angles; 45°, 60°, 90°.

3.5.3.1 Effect of porosity change

Similar to first two cases of baffle placements, there is little change to streamlines and temperature contours as shown in Figure 3.41 and 3.42. There is only a moderate difference to local Nusselt number at the location of the first baffle which is can be seen in 0.15 m position mark of Figure 3.43.

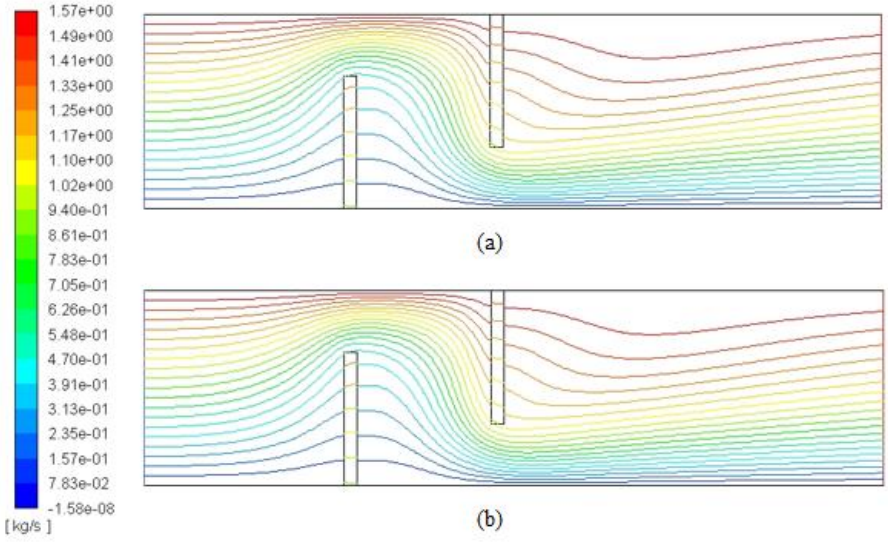

Figure 3.41 : Streamlines for two staggered baffles in channel with porosity values (a) 0.4 and (b) 0.9, respectively.

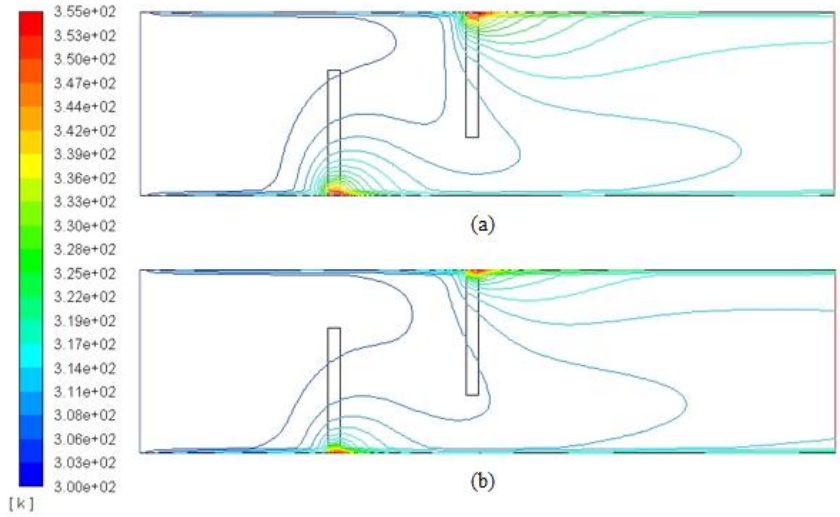

Figure 3.42 : Temperature contours for two staggered baffles in channel with porosity values (a) 0.4 and (b) 0.9, respectively.

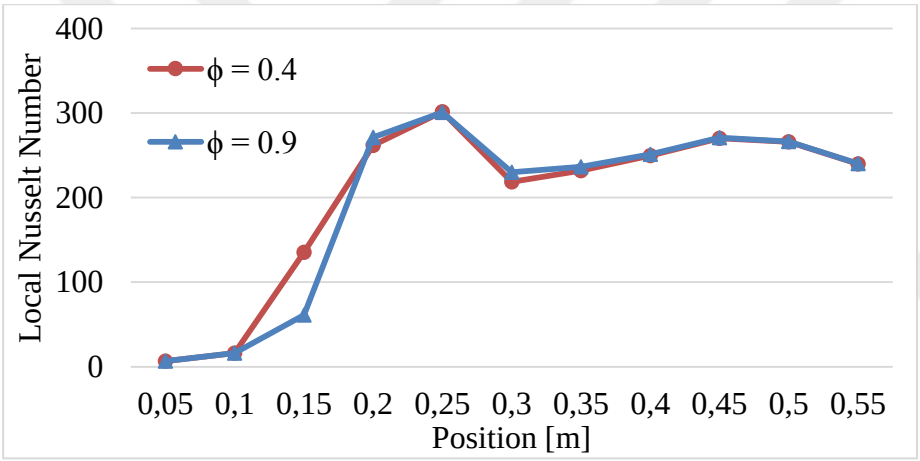

Figure 3.43 : Effect of baffle porosity on local Nusselt Number for two staggered baffles in channel with 90° inclination angle.

3.5.3.2 Effect of permeability change

Considering the same three alternative conditions for permeability, which are K = 1 × 10^{-9} m^2, K = 1 × 10^{-8} m^2, K = 1 × 10^{-7} m^2, similar results are obtained in terms of heat transfer trends. However, average values of local Nusselt values are lower than Case 2 and more similar to Case 1. On the other hand, there are minor differences in streamlines and temperature contours in Figures 3.44 and 3.45, as expected due to positioning of baffles. Figure 3.46 describes the results of heat transfer amount related to local Nusselt number. As expected from previous cases where the effect of permeability was investigated, there is very little disturbance to flow as seen from velocity and temperature profile curves in Figure 3.47 and Figure 3.48.

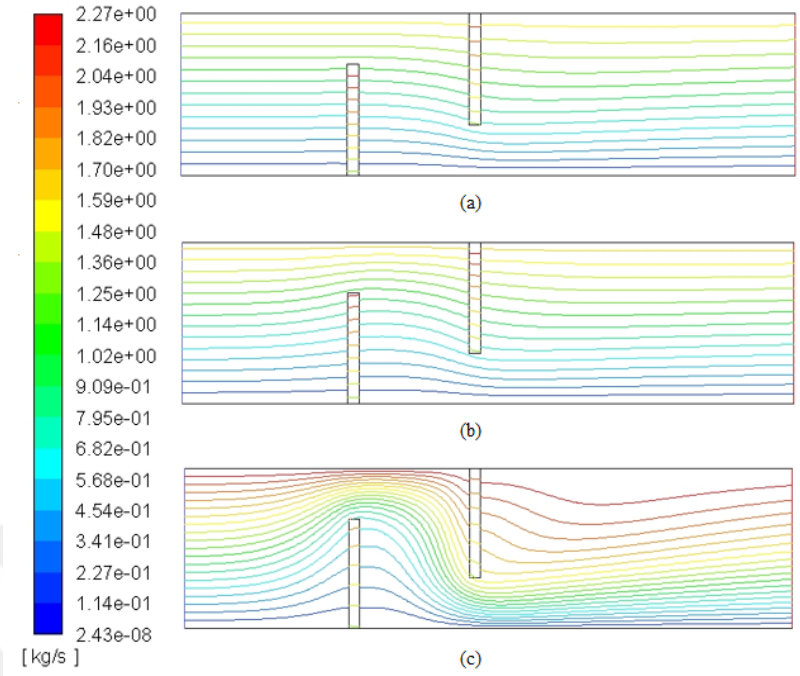

Figure 3.44 : Streamlines for two staggered baffles in channel with permeability values (a) K = 1×10^{-7} m^2, (b) K = 1×10^{-8} m^2, (c) K = 1×10^{-9} m^2, respectively.

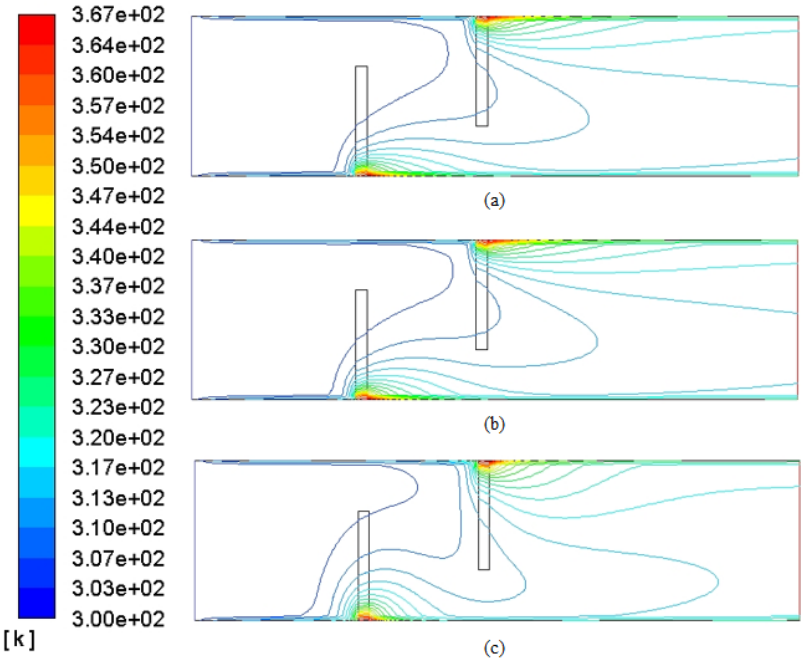

Figure 3.45 : Temperature contours for two staggered baffles in channel with permeability values (a) K = 1×10^{-7} m^2, (b) K = 1×10^{-8} m^2, (c) K = 1×10^{-9} m^2, respectively.

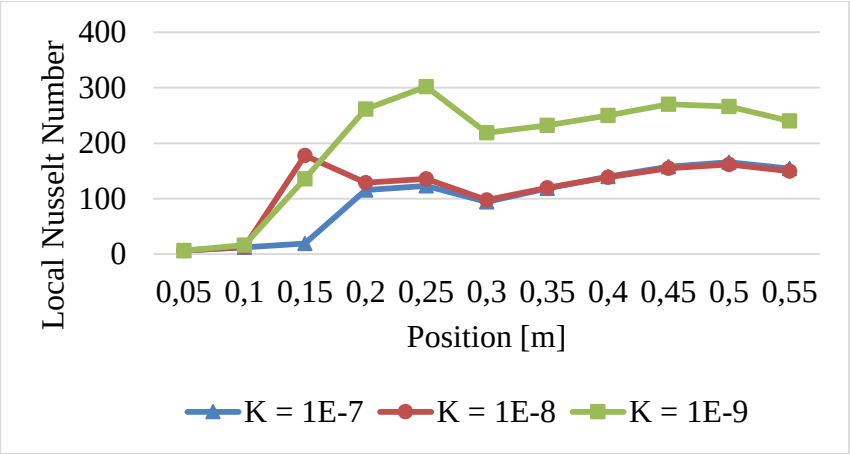

Figure 3.46 : Effect of baffle permeability on local Nusselt Number for two staggered baffles in channel with 90° inclination angle.

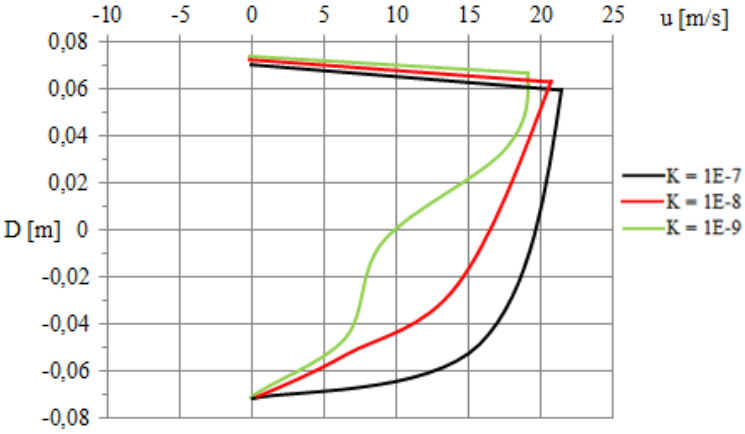

Figure 3.47 : Effect of baffle permeability on velocity profile for two staggered baffles in channel with 90° inclination angle.

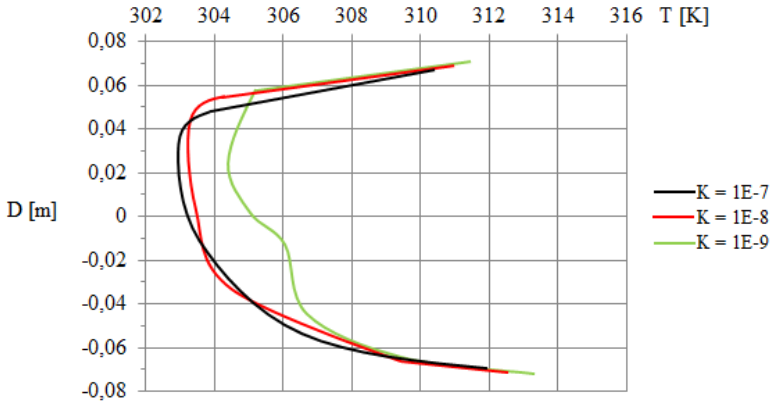

Figure 3.48 : Effect of baffle permeability on temperature profile for two staggered baffles in channel with 90° inclination angle.

3.5.4 Comparison of solid and porous baffles

An auxiliary study is conducted in order to see the difference between the porous model and a solid model which has a baffle without any porosity related features. For this analysis, channel dimensions are taken same as previous cases which were given in Table 3.2.

Similar to dimensional information, boundary conditions are also kept as before, given in Section 3.2.2. For the porous case, porosity characteristics of the baffle material are chosen as 0.4 for porosity and 10^{-9} for permeability. From the previous cases, it was shown that the best flow and heat transfer performance gain was for the cases where the inclination angle had increased. Therefore, this comparison study was performed for only the 90° single baffle condition.

For the solid case, it can be seen in Figure 3.49 that the streamlines are disturbed heavily and hence the flow can not develope quickly enough. On the contrary, porous baffle allows fluid flow through due to the nature of porous material; resulting in many advantages such as flow developing easier, lower pressure drop and so on. Furthermore, temperature concentration locations are also different for these two conditions as shown in Figure 3.50.

It should also be noted that the porous case has a higher singular temperature concentration than that of the solid case. Due to the fact that the flow can carry more heat through the channel with a porous baffle, heat transfer for this case looks more advantageous.

Finally, Figure 3.51 has the difference in velocity profile formations for two cases. One can see that the porous baffle allows flow to move with inreased velocity without turning to negative direction due to eddy formations. Additionally, flow becomes more developed in porous case. Temperature change between top and bottom is higher in porous case due to flow being more developed, as shown in Figure 3.52.

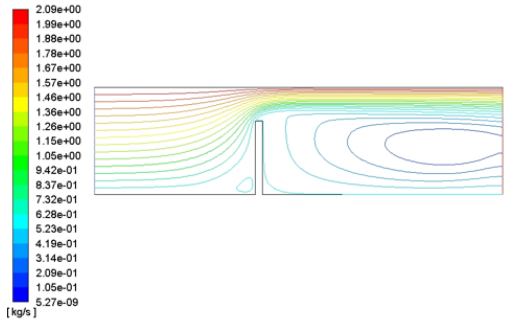

(a)

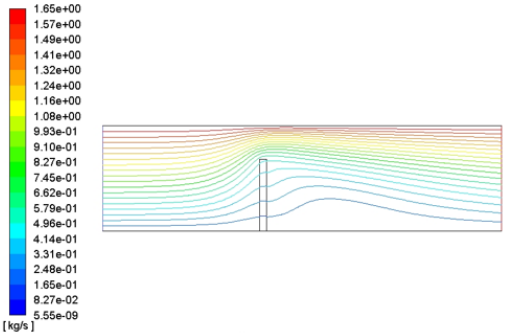

(b)

Figure 3.49 : Streamlines for a single baffle in channel with 90° inclination angle, for (a) solid and (b) porous cases.

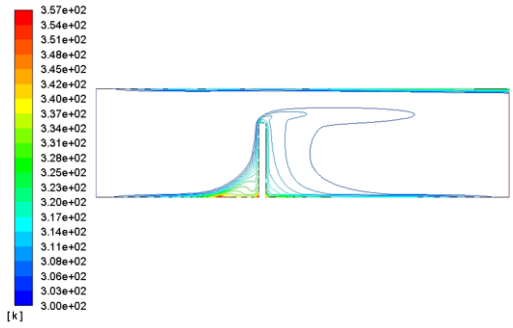

(a)

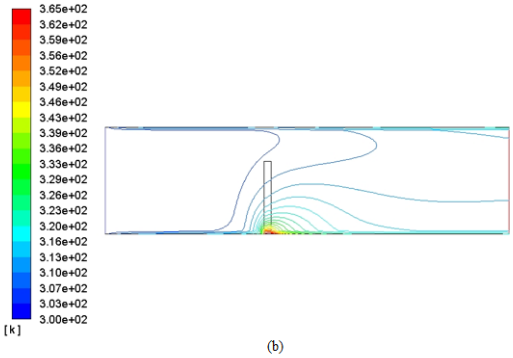

(b)

Figure 3.50 : Temperature contours for a single baffle in the channel with 90° inclination angle, for (a) solid and (b) porous cases.

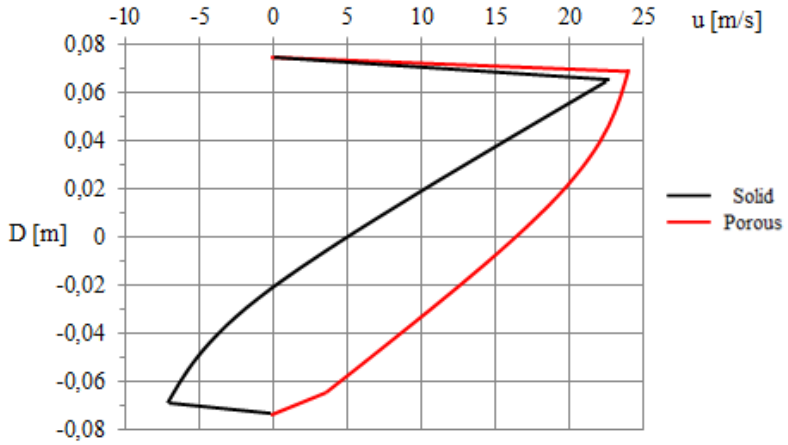

Figure 3.51 : Comparison of velocity profile formation for a single baffle in the channel with 90° inclination angle, for solid and porous cases.

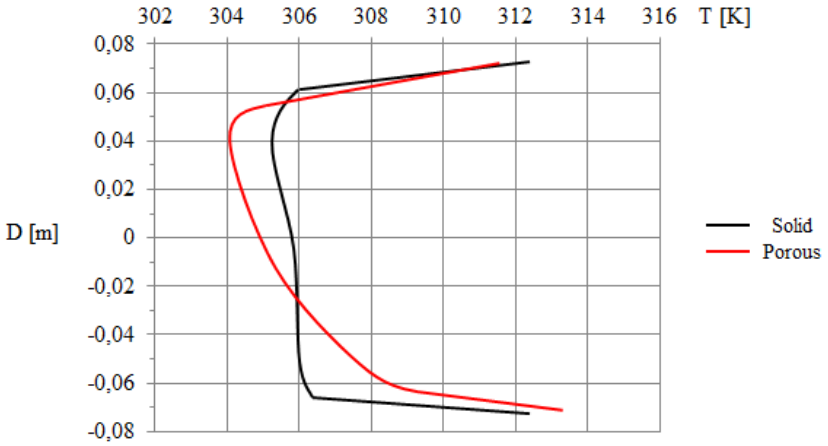

Figure 3.52 : Comparison of temperature profile formation for a single baffle in the channel with 90° inclination angle, for solid and porous cases.

4. CONCLUSIONS AND RECOMMENDATIONS

In this work, the effect of baffle inclination angle and formation in a channel flow was investigated; where the baffles with different permeability and porosity values were used. During the study, analyses were performed via ANSYS Fluent module and the results for flow characteristics, local Nusselt numbers, isotherms, velocity and thermal profiles of each case were shared and compared.

Comparison of three cases proves that either placed as staggered or tandem, adding a secondary baffle increases the average local Nusselt number throughout the channel. Once the flow reaches to first baffle, it becomes distracted by an amont depending on the baffle angle. It becomes squeezed and slows down between the channel walls if the baffle inclination angle is small, such as 45°. On the other hand; it can be seen that the local Nusselt number, hence the average heat transfer, is higher when the inclination angle of the baffle is greater; especially for Case 2. This is due to that the flow is less restricted, has higher velocity and adequate amount of recirculation. This idea can as well be supported by looking at the flow characteristics and increase in heat transfer close to the end of channel.

When the effect of porosity is inspected, one can end up with similar comments on the baffle placements as previously. However, it is clear that changing the porosity by proposed amount has little to no effect on heat transfer and flow characteristics.

One can see the effect of permeability in all three cases; as it plays an important role when the three cases of permeability values are compared and it seems to have a bigger control on the flow than porosity. Baffles with higher permeability show worse heat transfer performance that may be due to the lack of recirculation strength.

As in the case of solid and porous baffle comparison, porosity of a single baffle can positively affect the flow characteristics and carried amount of heat through the channel. When the flow encounters with the solid baffle, on the other hand, behaves in a more dispersed way; hence ending up with an increased amount of turbulence density.

For a further study, one can take a deeper look at the relation between permeability and recirculation; even performing analyses for comparison. Moreover, additional baffles and different types of placement can be analysed.

In terms of industrial usage, it can be said that there is a need for experimental studies in order to have a better correlation between computer aided simulation results. Additionally, adaptation of porous materials to the current manufacturing technologies of radiators and intercoolers is critical to applicability of this and other similar studies.

REFERENCES

Ait-Mokthar, A., Amiri, O. & Sammartinot, S. (1999). Analytic modelling and experimental study of the porosity and permeability of a porous medium-application to cement mortars and granitic rock. *Magazine of Concrete Research, 51,* 391-396.

Baytaş, A. C. (2006). Gözenekli ortamlarda taşınım olayı. *itü dergisi*, 4, 1, 3-13.

Darcy, H. (1856). *Fontaines Publiques de la Ville de Dijon*. Librairie des Corps Impériaux des Ponts et Chaussées et des Mines.

Ergün, S. (1952). Fluid flow through packed columns. *Chemical Engineering and Progress,* 8(2), 89-94.

Gaudillere, C. and Serra, J. M. (2016). Freeze-casting: fabrication of highly porous and hierarchical ceramic supports for energy applications. *Boletin de la Sociedad Española de Ceramica y Vidrio, 55,* 45-54.

Harpalani, S. and Chen, G. (1995). Estimation of changes in fracture porosity of coal with gas emission. *Fuel, 74,* 1491-1498.

Hwang, J.-J. (1997). Turbulent heat transfer and fluid flow in a porous-baffled channel. *Journal of Thermophysics and Heat Transfer, 11,* 429-436.

Ko, K.-H. and Anand, N. K. (2003). Use of porous baffles to enhance heat transfer in a rectangular channel. *International Journal of Heat and Mass Transfer, 46,* 4191-4199.

Li, H. Y., Leong, K. C., Jin, L. W. & Chai, J. C. (2010). Analysis of fluid flow and heat transfer in a channel with staggered porous blocks. *International Journal of Thermal Sciences, 49,* 1-24.

Louhibi, M. A., Salhi, N., Bouali, H., & Amghar, K. (2014). Numerical analysis of heat transfer in a channel with Inclined baffles, *International Journal of Engineering and Science, 4,* 12-23.

Mahadevan, S., Ricklick, M. & Kapat, J. S. (2013). Internal cooling using porous turbulators: heat transfer and pressure drop measurements. *Journal of Thermophysics and Heat Transfer, 27,* 526-533.

Naik, B. & Ghosh, N. N. (2009). A review on chemical methodologies for preparation of mesoporous silica and alumina based materials. *Recent Patents on Nanotechnology, 3,* 213-224.

Patankar, S. V. (1980). Numerical heat transfer and fluid flow. Retrieved from http://books.google.com/books (Original work published 1980)

Saar, M. O. and Manga, M. (1999). Permeability-porosity relationship in vesicular basalts. *Geophysical Research Letters, 26,* 111-114.

Santos, N. B. and de Lemos, M. J. S. (2006). Flow and heat transfer in a parallel-plate channel with porous and solid baffles. *Numerical Heat Transfer, 49,* 950-962.

Vafai, K. and Tien, C.L. (1981). Boundary and inertia effects on flow and heat transfer in porous media. *Inter. J. Heat and Mass Transfer, 28,* 1597-1611.

Yang, Y.-T. and Hwang, C.-Z. (2003). Calculation of turbulent flow and heat transfer in a porous-baffled channel. *International Journal of Heat and Mass Transfer, 46,* 771-780.

CURRICULUM VITAE

Name Surname **:** Ahmet Baş

Place and Date of Birth **:** 03.10.1990, Çankırı

E-Mail **:** basahmet90@gmail.com

EDUCATION :

- **B.Sc.** **:** 2013, Middle East Technical University, Department of Engineering, Mechanical Engineering

PROFESSIONAL EXPERIENCE AND REWARDS:

- Air Induction & Cooling Systems product development engineer in Ford Otosan AS since 08.07.2013.